Article type:

Submitted version – Preprint

Full citation:

Luca Piemontese, Carmen Cerchia, Antonio Laghezza, Pamela Ziccardi, Sabina Sblano, Paolo Tortorella, Vito Iacobazzi, Vittoria Infantino, Paolo Convertini, Fabrizio Dal Piaz, Angelo Lupo, Vittorio Colantuoni, Antonio Lavecchia,* Fulvio Loiodice*. New diphenylmethane derivatives as peroxisome proliferator-activated receptor alpha/gamma dual agonists endowed with anti-proliferative effects and mitochondrial activity. Eur. J. Med. Chem. 2017, 127, 379-397, DOI: 10.1016/j.ejmech.2016.12.047.

Publication History:

Received 5 October 2016, available online 24 December 2016, version of record 8 January 2017

Source name:
European Journal of Medicinal Chemistry
ISSN: 0223-5234
E- ISSN: 1768-3254

Editor:
Elsevier

Link for final version:
https://www.sciencedirect.com/science/article/abs/pii/S0223523416310534

New diphenylmethane derivatives as Peroxisome Proliferator-Activated Receptor alpha/gamma dual agonists endowed with anti-proliferative effects and mitochondrial activity

Luca Piemontese[a,b], Carmen Cerchia[c], Antonio Laghezza[a], Pamela Ziccardi[d], Sabina Sblano[a], Paolo Tortorella[a], Vito Iacobazzi[e,f], Vittoria Infantino[e,g], Paolo Convertini[e,g], Fabrizio Dal Piaz,[h] Angelo Lupo[d], Vittorio Colantuoni[d], Antonio Lavecchia[c,*] Fulvio Loiodice[a,*]

[a] *Dipartimento Farmacia-Scienze del Farmaco, Università degli Studi di Bari "Aldo Moro", via Orabona 4, 70125 Bari (Italy)*

[b] *Istituto di Scienze delle Produzioni Alimentari, Consiglio Nazionale delle Ricerche, via Amendola 122/O, 70126 Bari (Italy)*

[c] *Dipartimento di Farmacia, "Drug Discovery" Laboratory, Università degli Studi di Napoli "Federico II", via D. Montesano 49, 80131 Napoli (Italy)*

[d] *Dipartimento di Scienze e Tecnologie, Università degli Studi del Sannio, via Port'Arsa 11, 82100 Benevento (Italy)*

[e] *Dipartimento di Bioscienze, Biotecnologie e Biofarmaceutica, Laboratorio di Biochimica e Biologia Molecolare, Università degli Studi di Bari "Aldo Moro", via Orabona 4, 70125 Bari (Italy)*

[f] *Istituto di Biomembrane e Bioenergetica, Consiglio Nazionale delle Ricerche, via Orabona 4, 70125 Bari (Italy)*

[g] *Dipartimento di Scienze, Università della Basilicata, viale dell'Ateneo Lucano 10, 85100 Potenza (Italy)*

[h] *Dipartimento di Medicina e Chirurgia, Università di Salerno, via Giovanni Paolo II 132, 84084 Fisciano, SA, (Italy)*

Corresponding Authors: Prof. Fulvio Loiodice, Dipartimento di Farmacia-Scienze del Farmaco, Università degli Studi di Bari "Aldo Moro", Via Orabona 4, 70126 Bari, Italy; phone: +39 080-5442778, e-mail: fulvio.loiodice@uniba.it; Prof. Antonio Lavecchia, Dipartimento di Farmacia, "Drug Discovery" Laboratory, Università degli Studi di Napoli "Federico II", Via Domenico Montesano 49, 80131 Napoli, Italy; phone: +39 081-678613, e-mail: antonio.lavecchia@unina.it.

Abbreviations: PPAR, peroxisome proliferator-activated receptor; LBD, ligand binding domain; TZDs, thiazolidinediones; CAC, carnitine/acylcarnitine carrier; CPT1, carnitine-palmitoyl-transferase 1; PGC-1α, peroxisome proliferator-activated receptor gamma coactivator 1-alpha; SPR, Surface Plasmon Resonance.

Abstract

We screened a short series of new chiral diphenylmethane derivatives and identified potent dual PPARα/γ partial agonists. As both enantiomers of the most active compound **1** displayed an unexpected similar transactivation activity, we performed docking experiments to provide a molecular understanding of their similar partial agonism. We also evaluated the ability of both enantiomers of **1** and racemic **2** to inhibit colorectal cancer cells proliferation: (*S*)-**1** displayed a more robust activity due, at least in part, to a partial inhibition of the Wnt/β-catenin signalling pathway that is upregulated in the majority of colorectal cancers. Finally, we investigated the effects of (*R*)-**1**, (*S*)-**1** and (*R,S*)-**2** on mitochondrial function and demonstrated that they activate the carnitine shuttle system through upregulation of carnitine/acylcarnitine carrier (CAC) and carnitine-palmitoyl-transferase 1 (CPT1) genes. Consistent with the notion that these are PPARα target genes, we tested and found that PPARα itself is regulated by a positive loop. Moreover, these compounds induced a significant mitochondrial biogenesis. In conclusion, we identified a new series of dual PPARα/γ agonists endowed with novel anti-proliferative properties associated with a strong activation of mitochondrial functions and biogenesis, a potential therapeutic target of the treatment of insulin resistance.

Keywords: PPAR, docking experiments, mitochondrial biogenesis, anti-proliferative effects, gene expression analysis.

1. Introduction

Peroxisome proliferator-activated receptors (PPARs) are ligand-activated transcription factors belonging to the nuclear hormone receptor superfamily. The interaction with specific ligands of these receptors elicits a conformational change of the ligand binding domain (LBD) that allows the recruitment of coactivators on the promoter regions of target genes. The enhanced expression of these genes is directly or indirectly involved in energy homeostasis, lipid and carbohydrate metabolism.[1-6] Three PPAR subtypes (designated α, γ and δ) have been identified so far with different tissue distribution and ability to modulate diverse physiological functions. The activation of PPARα by hypolipidemic agents (e.g. fenofibrate) stimulates fatty acid β-oxidation, increases high density lipoprotein (HDL), and decreases very low and low density lipoproteins (VLDL and LDL) in blood.[7,8] The thiazolidinedione (TZD) class of antidiabetic agents (rosiglitazone, pioglitazone) are PPARγ agonists [9] acting as insulin sensitizers in target tissues and lowering glucose and fatty acid levels in type 2 diabetic patients. However, despite their proven benefits, PPARγ full agonists possess a number of deleterious side effects such as weight gain, peripheral edema, increased risk of congestive heart failure and higher rate of bone fracture.[10-13] Recently, one of the most prescribed TZD, rosiglitazone, has been withdrawn from the market by the EMEA and european patients have been forced to change their antidiabetic therapy.[14] For this reason, the current therapeutic frontier is to search for PPARγ partial agonists or modulators that retain the therapeutic activity while displaying reduced adverse effects.[15-17] PPARδ, albeit ubiquitously expressed, has functions not fully elucidated. Recent studies have identified a role in cholesterol metabolism, adipocyte differentiation, neuronal function and colon cancer.[18] To date, no PPARδ agonist has been developed and the clinical potential of its therapeutic targeting remains to be clearly determined.

In line with this reasoning, in the last few years many efforts have been directed toward the design of new molecules that combine the insulin-sensitizing effect of PPARγ and the additional

lipid-modifying activity of PPARα. In fact, the development of dual PPARα/γ agonists has been considered a very attractive option in the treatment of dyslipidemic type 2 diabetes.[19-20] A number of drugs acting as full PPARα agonists and partial PPARγ agonists have recently been developed. However, except for saroglitazar, which has recently been approved in India for the treatment of diabetic dyslipidemia and hypertriglyceridemia with type 2 diabetes not controlled by statin therapy,[21] none of them has progressed further to preclinical or phase II trials.

In search for novel pharmacophores able to provide a suitable dual activation of these PPAR subtypes, we designed a new class of ligands characterized by the presence of the 2-oxy-propanoic acid moiety linked to the diphenylmethane skeleton that has already shown its usefulness as a multi-template for nuclear receptors.[22-24] The diphenylmethane skeleton was fused, through an oymethylene linker, with the 2-phenyl-1,3-oxazole nucleus that is typical of a number of PPARα/γ agonists.[25] The combination of these two structural moieties provided compounds **1** and **2** (Figure 1). With the aim to obtain compounds endowed with activity also toward the farnesoid X receptor (FXR), we introduced into the structure of **1** and **2** some chemical modifications similar to those reported in some diphenylpentane-based phenoxyacetic acids acting as FXR agonists.[24] Modulation of FXR may be a valuable therapeutic approach for various pathophysiological conditions. In particular, FXR activation showed promising results in vitro and in vivo for the treatment of metabolic diseases such as type 2 diabetes.[26-28]

To this goal, we investigated the effects on the activity of **1** and **2** originating from the presence of two chlorine atoms on the ortho position of the distal aromatic ring, of a methyl on the oxazole nucleus, and of two ethyl groups on the benzylic carbon. In this way, we prepared the diphenylpentane derivatives **3-6** displayed in Figure 1. In addition, considering the well-known sensitivity of PPARs to stereochemistry, we explored the influence of absolute configuration on receptor activation.

In the present series, only diphenylmethane derivatives showed potent dual PPARα/γ

agonist activity with a 20-40% efficacy with respect to reference compounds. Surprisingly, both enantiomers of the most active compound **1** displayed similar activity. Docking experiments were performed to provide a molecular explanation for this unexpected effect and also to rationalize the lack of activity of diphenylpentane derivatives. In addition, we tested whether both enantiomers of **1** and racemate **2** were endowed with an antiproliferative activity mediated by PPARγ. This was in line with the large body of data showing such a ligand-directed function in cells in vitro and in animal models in vivo.[29-33] Furthermore, we investigated whether (*S*)-**1** and (*R*)-**1** could affect mitochondrial carnitine/acylcarnitine carrier (CAC) and carnitine-palmitoyl-transferase 1 (CPT1) gene expression. These are two components of the carnitine shuttle system essential for fatty acids mitochondrial transport and subsequent β-oxidation. Transcription of the CAC gene has recently been shown to be enhanced by statins and fibrates, providing a novel contribution to the understanding of their hypolipidemic action.[34-37] Finally, we evaluated the effect of (*R*)-**1**, (*S*)-**1** and (*R,S*)-**2** on mitochondrial biogenesis. In fact, the increase of mitochondrial mass and oxidative activity is currently viewed as a potential therapeutic approach for the treatment of insulin resistance.

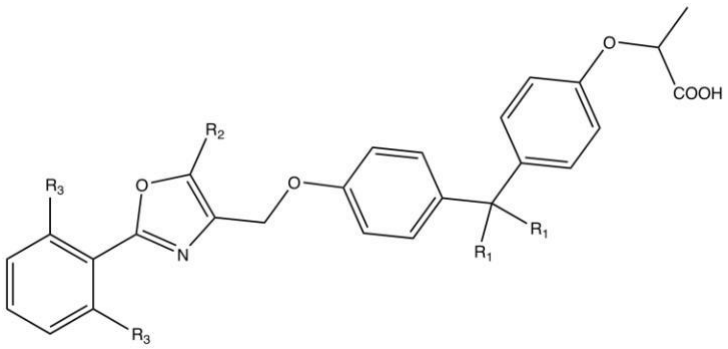

Compound	R_1	R_2	R_3
1	H	H	H
2	H	CH_3	H
3	C_2H_5	H	H
4	C_2H_5	CH_3	H
5	C_2H_5	H	Cl

6	C_2H_5	CH_3	Cl

Figure 1. Diphenylmethane derivatives reported in the present study.

2. Chemistry

The synthesis of compounds **1-6** started with the preparation of the intermediates **7-11** (Scheme 1). The condensation of benzamide or 2,6-dichlorobenzamide with 1,3-dichloroacetone, in a vial at 180 °C gave compounds **7** and **8**, respectively. Compounds **9-10** were obtained by condensation of butan-2,3-dione with hydroxylamine hydrochloride in the presence of sodium acetate and subsequent reaction with benzaldehyde or 2,6-dichloro-benzaldehyde. The final treatment with $POCl_3$ allowed to obtain the target intermediates. Finally, the reaction between phenol and 3-pentanone in the presence of methansulfonic acid gave the intermediate **11**.

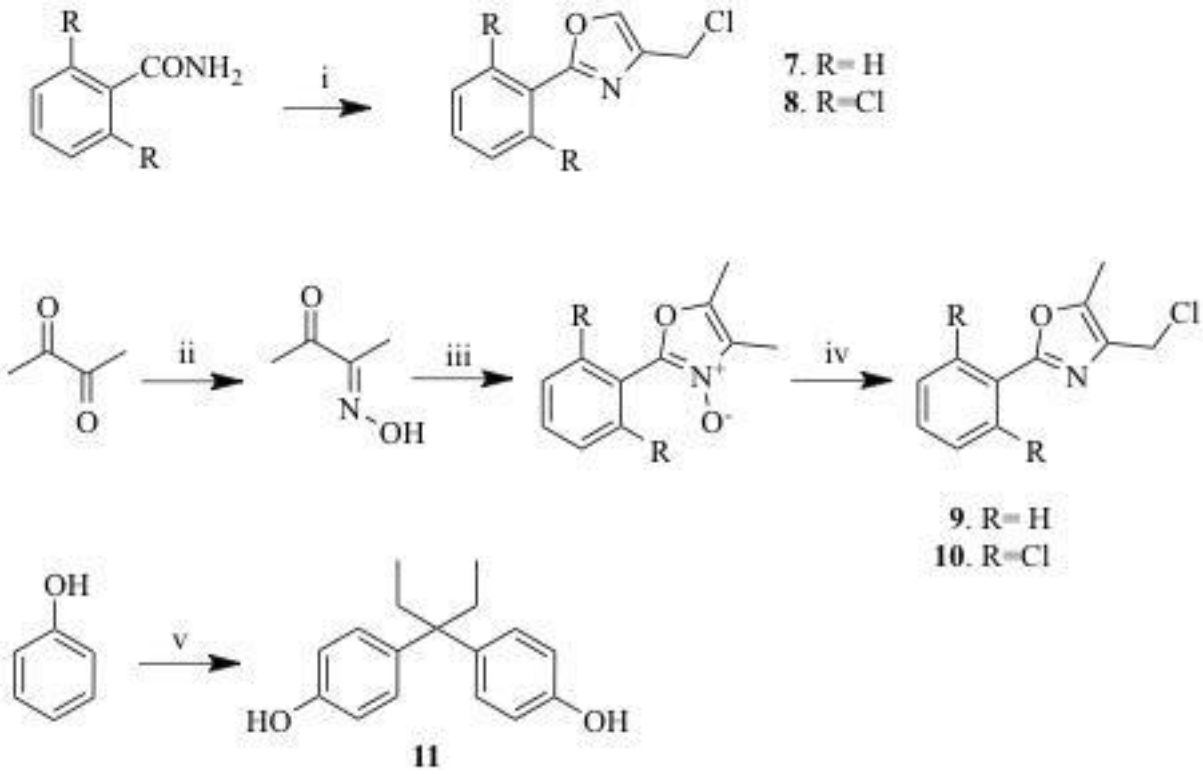

Scheme 1. i) 1,3-dichloroacetone, 180 °C; ii) $NH_2OH{\cdot}HCl$, CH_3COONa, $EtOH/H_2O$, rt; iii) benzaldheyde or 2,6-dichlorobenzaldheyde, 4M HCl/dioxane, rt; iv) $POCl_3$, anhydrous $CHCl_3$, reflux; v) 3-pentanone, methansulfonic acid, rt.

The reaction of the commercially available bis(4-hydroxyphenyl)methane or **11** with ethyl or methyl 2-bromopropionate in the presence of Cs_2CO_3 led to compounds **12-13**. These derivatives were condensed with the intermediates **7-10** in the presence of NaH to give esters **14-19** whose alkaline hydrolysis afforded the target acids **1-6** (Scheme 2).

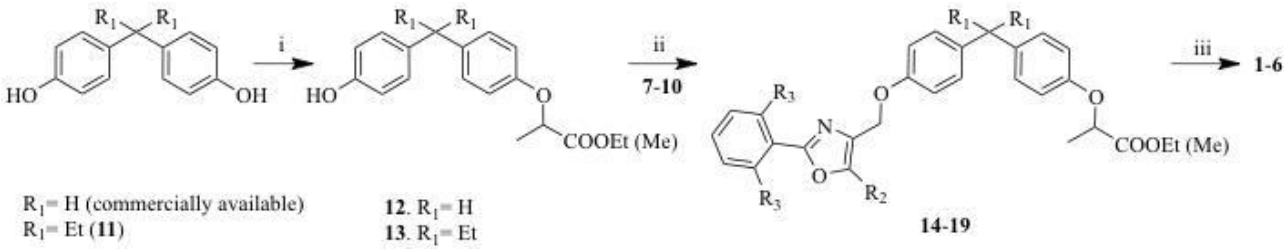

Scheme 2. i) ethyl or methyl 2-bromopropionate, Cs_2CO_3, acetonitrile, reflux; ii) 95% NaH, anhydrous THF, reflux; iii) 1N NaOH, THF, rt.

The synthesis of the enantiomers of **1** started with the condensation between bis(4-hydroxyphenyl)methane and (*R*)- or (*S*)-methyl lactate via a Mitsunobu reaction which is known to occur with inversion of configuration. The so obtained methyl esters (*R*)-**12** and (*S*)-**12** were condensed with **7** following the same procedure shown in scheme 2 which finally afforded the target acids (*R*)-**1** and (*S*)-**1** (Scheme 3).

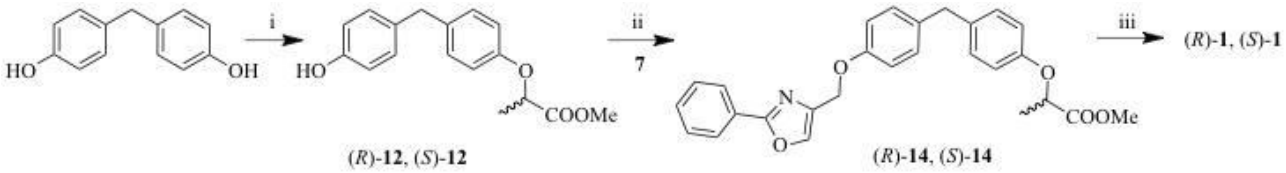

Scheme 3. i) (*R*)- or (*S*)-methyl lactate, DIAD, triphenylphosphine, anhydrous THF, rt; ii) 95% NaH, anhydrous THF, reflux; iii) 1N NaOH, THF, rt.

3. Results and discussion

Compounds **1-6** were evaluated for their agonist activity toward the human PPARα (hPPARα), PPARγ (hPPARγ), PPARδ (hPPARδ), and FXR (hFXR) subtypes. For this purpose, GAL4-PPAR or GAL4-FXR chimeric receptors were transiently transfected in HepG2 cells according to a previously reported procedure.[38] The results were compared with those obtained with Wy-14,643, rosiglitazone, L-165,041, and chenodeoxycholic acid used as reference compounds for PPARα, PPARγ, PPARδ, and FXR respectively (Table 1). Maximum fold induction obtained with the reference agonist was set at 100%.

Table 1. Activity of the tested compounds in a cell-based transactivation assay.

	PPARα		**PPARγ**		**PPARδ**	
Cpd	**EC_{50} (μM)**	**E_{max}** [a]	**EC_{50} (μM)**	**E_{max}** [a]	**EC_{50} (μM)**	**E_{max}** [a]
1	0.039±0.013	47±13	0.29±0.08	26±3	nc	15
(*S*)-1	0.046±0.023	39±3	0.30±0.21	17±5	nc	11
(*R*)-1	0.042±0.031	44±9	0.28±0.16	26±4	nc	14
2	0.100±0.010	34±14	0.29±0.06	20±3	nc	13
3	nc	40	nc	10	ia	ia
4	nc	17	nc	3	ia	ia
5	nc	18	nc	10	ia	ia
6	nc	24	nc	9	ia	ia
Wy-14,643	1.6±0.3	100±10	ia	ia	ia	ia
Rosiglitazone	ia	ia	0.04±0.02	100±9	ia	ia
L-165,041	ia	ia	ia	ia	0.02±0.002	100±4

[a]Efficacy values were calculated as the percentage of the maximum obtained fold induction relative to the reference compounds. ia = inactive at tested concentrations (up to 2 μM). nc = not computable; the activity, in fact, increases with increasing concentrations up to 2 μM, above which the activity begins to decrease.

Unexpectedly, all compounds exhibited no activity on FXR (data not shown), whereas most compounds displayed partial agonism on PPARs. Specifically, compound **1** turned out to be a potent partial agonist on PPARα and PPARγ subtypes; at higher doses it showed moderate activity even on PPARδ; above 2 μM the activity started to decline due to the toxicity toward the cell line employed in the assay. The presence of an additional methyl group on the oxazole ring (compound **2**) did not significantly affect the activity, which resulted 2.5 times lower than **1** only on PPARα. The introduction of the ethyl groups on the methylene bridge between the two phenyl rings (compounds **3** and **4**) as well as the presence of two chlorine atoms on the distal benzene linked to oxazole (compounds **5** and **6**) dramatically reduced the activity. In fact, PPARα and PPARγ activity only marginally increased upon exposure to increasing concentrations of these compounds up to 2 μM, above which the activity started to decrease due to cytotoxicity. By contrast, no activity was detected toward the PPARδ subtype. On the whole, **1** turned out to be the one with the best pharmacological profile. For this reason, we decided to prepare its stereoisomers to evaluate whether the absolute configuration of the stereocenter close to the carboxylic function could affect the activity. Surprisingly, (*R*)-**1** and (*S*)-**1** displayed the same effects toward all PPAR subtypes. To evaluate if the observed results were dependent upon the direct interaction of (*R*)-**1** and (*S*)-**1** with the receptors, we performed a surface plasmon resonance (SPR) assay; different concentrations of the two stereoisomers were injected on each of the three PPAR subtypes, singularly immobilized on sensor chips.[39] Wy-14,643, rosiglitazone and L-165,041 were used as controls. The results clearly indicated a high affinity of (*R*)-**1** and (*S*)-**1** towards PPARα (Figure 2 and Table 2); both compounds also effectively bound PPARγ , whereas no interaction with PPARδ was observed.

Table 2. Thermodynamic (K_D) and kinetics (K_d) dissociation constants measured by SPR for the interaction of the stereoisomers of **1** with PPAR subtypes.

	PPARα		PPARγ		PPARδ	
Cpd	**K_D (nM)**	**K_d (s^{-1})**	**K_D (nM)**	**K_d (s^{-1})**	**K_D (nM)**	**K_d (s^{-1})**
(*S*)-1	0.75±0.18	0.016±0.009	4.9±1.1	0.099±0.023	n.b.	n.b.
(*R*)-1	0.86±0.11	0.025±0.007	3.7±0.5	0.095±0.016	n.b.	n.b.
Wy-14,643	18.9±5.6	0.36±0.12	1297.3±19.6	2.3±0.6	n.b.	n.b.
Rosiglitazone	n.b.	n.b.	1.2 ±0.7	0.145±0.030	n.b.	n.b.
L-165,041	n.b.	n.b.	n.b.	n.b.	76.4±6.1	0.43±0.08

n.b. = no binding observed.

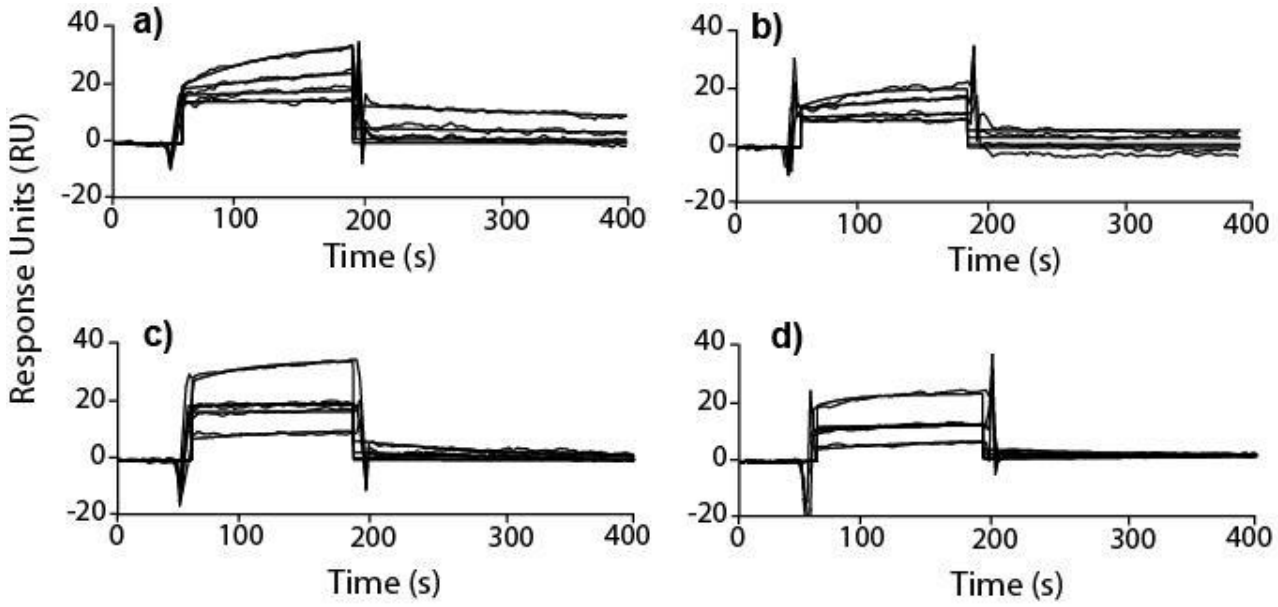

Figure 2. SPR sensorgrams resulting from the injection of different amounts of compounds (*R*)-**1** and (*S*)-**1** on immobilized PPARα (**a** and **b**), and PPARγ (**c** and **d**).

A comparison between SPR and the cell-based assay data indicates that the transactivation of PPARα and PPARγ by (*R*)-**1** and (*S*)-**1** depends on a direct interaction of these compounds with the two PPAR subtypes. Moreover, SPR results show a very similar behavior from the two stereoisomers towards the two receptors, both in terms of thermodynamic stability of the resulting

complexes, as inferred by the comparable K_Ds measured, and in terms of binding mode, as suggested by the observed K_ds.[40]

In order to rationalize the unexpected similar activity displayed by (*R*)-**1** and (*S*)-**1** toward all PPAR subtypes and to explain the lack of activity of diphenylpentane derivatives **3-6**, we performed docking experiments.

4. Docking calculations

In an effort to understand the molecular basis for the observed partial agonism of (*S*)-**1** and (*R*)-**1** toward both PPARα and PPARγ, we undertook docking studies using GOLD 5.2.2 program [41] in combination with the ChemPLP [42] scoring function (rescoring with ChemScore).[43] Docking experiments were carried out into the X-ray crystal structures of PPARγ ligand binding domain (LBD) complexed to partial agonist LT127 (PDB code: 2I4P) [44] and the PPARα LBD complexed to partial agonist aleglitazar (PDB: 3G8I).[45] The docking experiments predicted that both (*S*)-**1** and (*R*)-**1** enantiomers favorably bind to PPARγ LBD, adopting a similar U-shaped conformation that wraps around H3. Figure 3a,b clearly illustrates the binding poses of (*S*)-**1** and (*R*)-**1**, that appear almost identical when the LBD is superposed (Figure 3c). Superimposition of the two enantiomers on the co-crystal structure of full agonist rosiglitazone bound to PPARγ LBD (PDB code: 2PRG) revealed that the ligands do not make direct contact with residue Y473 in the activation function (AF-2) domain located on H12, like other partial agonists including GW0072 and nTZDpa (Figure 3d). The location of the polar carboxylate group is too far away from the H12 in comparison to the thiazolidinedione moiety of rosiglitazone. The carboxylate group of both (S)-**1** and (R)-**1** forms H-bonds with Y327 OH, H323 $N^{\varepsilon 2}$, and S289 OH atoms (Figure 3a,b), while the ether oxygen of the ligands forms an additional H-bond with S289 OH. The remainder structure wraps around H3 and buries the 2-phenyloxazole tail into a lipophilic pocket formed by H3, H5, the

β-sheet and the Ω-loop, a flexible loop region that links H2' to H3. (*S*)-**1** and (*R*)-**1** make important hydrophobic interactions with residues K265, G284, F287, C285, H266, R288, L330, L333, I341, and S342. The central phenoxy oxygen accepts a H-bond from the backbone NH of S342 side chain located within the β-sheet region of the receptor. In addition, the distal ring of 2-phenyloxazole tail appears to be optimally oriented for a favorable π–π stacking interaction with F287 positioned on H3, which contributes to further increase H3 stabilization. The lack of interactions with the AF-2 and the indirect stabilization of the PPARγ AF-2 surface via the alternative regions could provide the structural basis for the partial agonist properties of compounds (*S*)-**1** and (*R*)-**1**. Co-crystallography, mutagenesis and hydrogen/deuterium exchange (HDX) studies have all displayed that PPARγ full agonists activate the receptor through direct interactions with the Y473 residue located in the AF2 domain of H12 of the receptor [46] so to induce conformational changes that facilitate the recruitment of coactivators and hence transcriptional activation. In contrast, both enantiomers bind in the entry-end of the ligand-binding pocket at a distance from H12 that precludes direct contact with Y473. Rather, the high-affinity interactions between the two ligands and receptor originate from a direct H-bond with the main-chain NH of S342 of the β-sheet and from the numerous hydrophobic van der Waals contacts with residues of H3 and Ω-loop. These interactions could provoke destabilization of H12 and stabilization of H3 affecting the recruitment of coactivators and, in turn, PPARγ transactivation potential,[46,47] possibly explaining the partial agonism of (*S*)-**1** and (*R*)-**1** ligands.

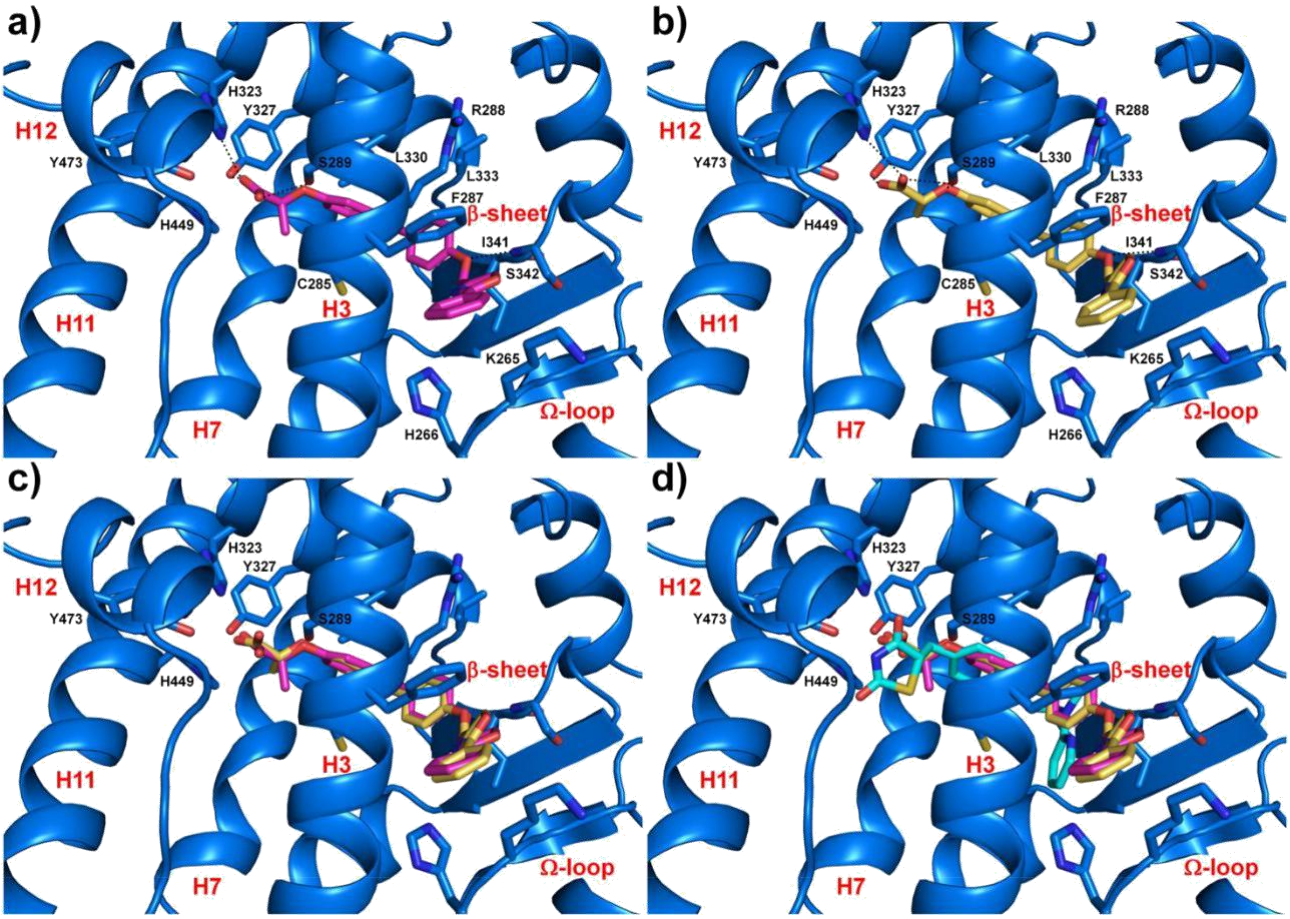

Figure 3. a) Binding mode of enantiomer (*S*)-**1** (magenta sticks) into the PPARγ binding site represented as a bluemarine ribbon model. b) Binding mode of enantiomer (*R*)-**1** (yellow sticks) into the PPARγ binding site. c) C^{α} superposition of the complexes of PPARγ with (*S*)-**1** and (*R*)-**1**. d) C^{α} superposition of the complexes of PPARγ with (*S*)-**1**, (*R*)-**1** and rosiglitazone (cyan sticks, PDB code 2PRG). Only amino acids located within 4 Å of the bound ligand are displayed (bluemarine sticks) and labeled. The Ω-loop, a flexible loop region between H2' and H3, and the β-sheet region of the LBD, are displayed. H-bonds discussed in the text are depicted as dashed black lines.

Similar docking experiments were undertaken to gain insight into the possible binding mode of (*R*)-**1** and (*S*)-**1** to PPARα LBD. An extensive survey of reported X-ray crystal structures of ligands complexed with PPARα LBD [45,48] shows that one or two water molecules bridge the T279 OH group on H3 with the A333 NH or L331 C=O backbone on the β-sheet, mediating contacts between H3 and β-sheet, likely stabilizing the structure of the receptor LBD. As two intervening water molecules are also present in the aleglitazar/PPARα complex and facilitate H-bonds between the two regions stabilizing the LBD, both water molecules were included in the docking experiments.

Both (*R*)-**1** and (*S*)-**1** enantiomers fit well within the PPARα binding pocket. As expected, the carboxylate head group, together with the ether oxygen, form the well recognized H-bonding network with residues H440, Y464, Y314, and S280, which is believed to be critical for PPARα ligands activity (Figure 4). In addition to these standard carboxylate interactions with the binding pocket, two further H-bonds are also observed: one between the central phenoxy oxygen and T279

OH group and the other between the oxazole nitrogen and the NH backbone of A333 on the β-sheet. It is noteworthy that the OH group of T279 makes an indirect H-bond with the L331 C=O backbone via two water molecules, thereby further stabilizing the β-sheet region of PPARα. The remaining interactions between ligand and protein are hydrophobic in nature; in particular, the methyl group binds into a hydrophobic pocket defined by F273, C276, Q277, I354, and V444, while the benzylphenoxy moiety is surrounded by hydrophobic residues V324, L321, I354, and three sulfur-containing amino acids, C276, M355, and M330, which form strong attractive sulfur-arene interactions;[49] the 2-phenyloxazole tail makes a good fit into the lower part of the binding pocket and would be expected to positively contribute to overall binding through van der Waals interactions with the hydrophobic residues L258, V255, A333, Y334, and C275. All these data support that (*R*)-**1** and (*S*)-**1** act as partial PPARα agonists and suggest that their binding induces conformational changes in the receptor LBD resulting in a distinct pattern of cofactor recruitment and selective gene induction ability.

Finally, docking experiments were also carried out to rationalize the lack of activity of compounds **3**-**6** toward either PPARα and PPARγ subtypes. The introduction of two bulky ethyl groups on the methylene bridge between the two phenyl rings was not tolerated due to severe steric clashes with specific residues (C285 and M364 for PPARγ; and L321, I354 and K358 for PPARα) present in the corresponding PPAR binding cleft. These results explicitly account for the lack of ability of **3**-**6** to bind PPARα and PPARγ.

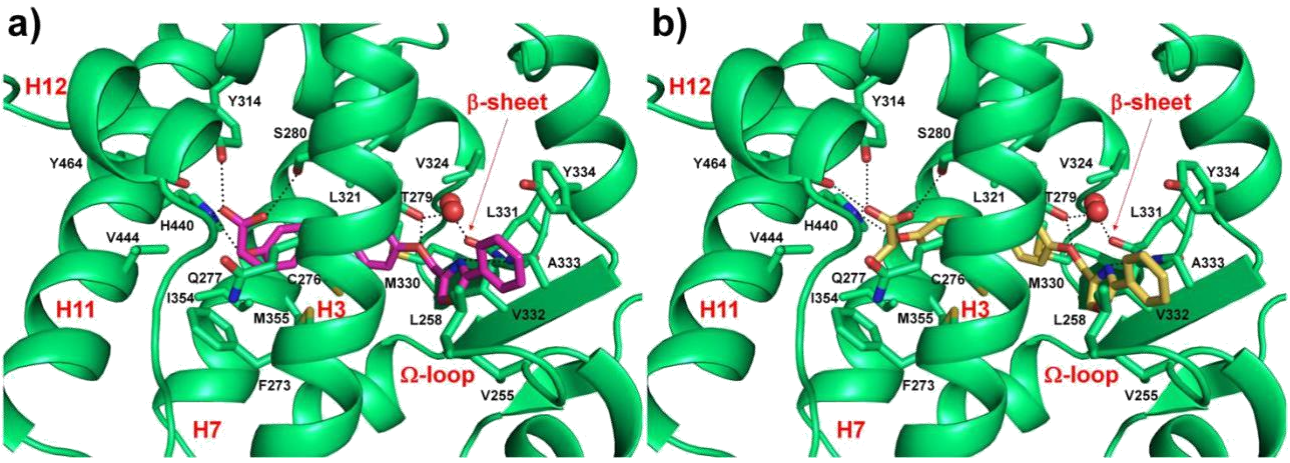

Figure 4. a) Binding mode of enantiomer (*S*)-**1** (a, magenta sticks) and (*R*)-**1** (b, yellow sticks) into the PPARα binding site represented as a green ribbon model. Only amino acids located within 4 Å of the bound ligand are displayed (green sticks) and labeled. The Ω-loop, a flexible loop region between H2' and H3, and the β-sheet region of the LBD, are displayed. The ordered water molecules bridging the T279 OH group on H3 and the L331 C=O backbone on β-sheet are displayed as red spheres. H-bonds discussed in the text are depicted as dashed black lines.

5. Compounds (*S*)-1, (*R*)-1 and (*R,S*)-2 inhibit the growth of the human CRC cell line HT29

Having all compounds of this series displayed cytotoxicity in the transactivation assays, we decided to evaluate their antiproliferative activity on a different cell type such as the colon cancer derived HT-29 cells which express PPARγ at high levels [38d] and assess differences between full and partial PPARγ agonists. This last point may be relevant as the antiproliferative activity, and thus the antineoplastic benefits, of the full agonists TZDs have produced so far conflicting results in clinical trials, justifying the need to further investigate the anticancer potential of novel PPARγ agonists.[50] For this purpose, we chose both enantiomers of **1** and racemic **2** and compared their activity with that of the full agonist rosiglitazone (Figure 5).

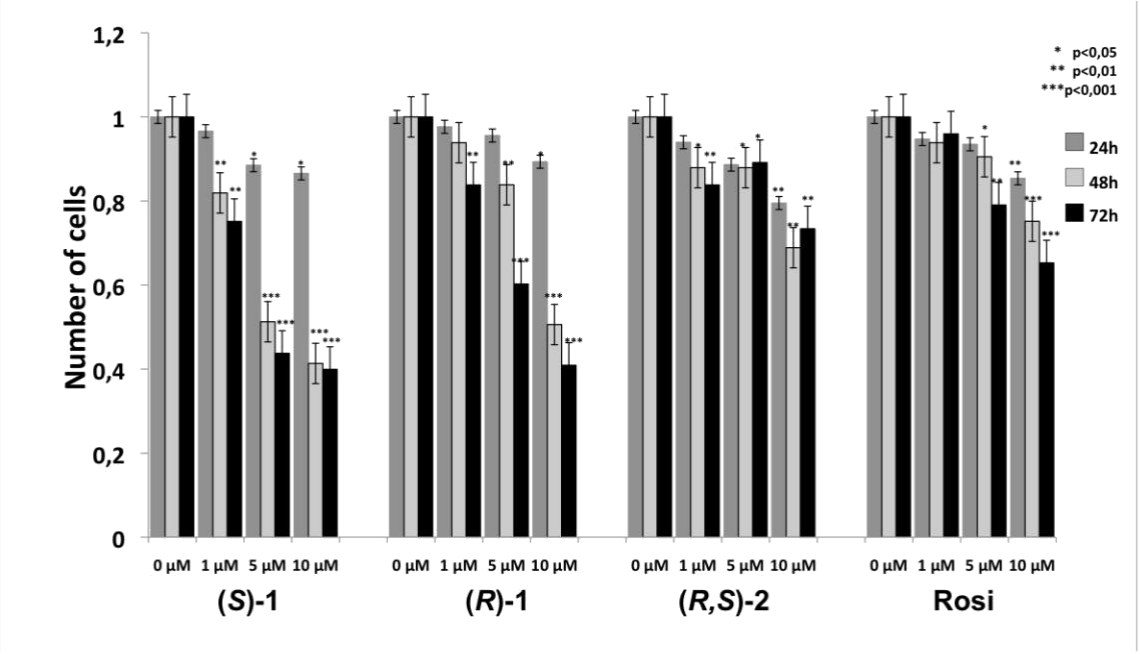

Figure 5. Evaluation of the antiproliferative potential of (*S*)-**1**, (*R*)-**1** and (*R,S*)-**2** in colon cancer cells. To assess the effect of the different compounds, exponentially growing HT-29 cells were exposed to vehicle alone or to 1, 5 and 10 μM of each drug for 24, 48 and 72 hs, collected and counted. The data shown here are the mean ± SD of three independent experiments performed in duplicate. Results were similar in three independent experiments. * $p < 0.05$, ** $p < 0.01$, *** $p < 0.001$, respectively, when compared to control.

The (*S*)-**1** compound elicited a robust antiproliferative activity that was dose- and time-dependent reaching the maximum (40% of residual cell vitality) between 5 and 10 μM at 72 hs. (*R*)-**1** also exhibited a dose- and time-dependent activity that was, however, less pronounced than (*S*)-**1**: the residual cell vitality upon 5 μM (*S*)-**1** treatment was about 45% as compared with 60% obtained with (*R*)-**1**. The even stronger effect obtained with 10 μM (*S*)-**1** and (*R*)-**1** at 72 hs may be partially referred to cytotoxic effects. The most striking result obtained in this experimental setting was the different growth inhibitory effect of (*S*)-**1** with respect to the racemic compound **2** and the full agonist rosiglitazone: the residual cell vitality obtained with these two latter compounds at 72 hs was, in fact, higher than the (*S*)-**1** enantiomer (70% and 65% vs 40% respectively).

We further investigated the cytotoxic effects of both enantiomers of **1** and racemic **2** in HEK293T, a cell line derived from a human embryonic kidney immortalized by transformation with adenovirus 5 DNA expressing a transfected SV40 large T antigen and generally considered as a normal cell line. Exposure to (*S*)-**1** (10 μM) for 48 hs elicited in HEK293T an antiproliferative effect that was

milder (about 75 % of cells were viable) than HT-29 cells (about 40 % of cells were viable) treated in parallel (Figure 6A). To confirm these data, in both cellular types, we investigated $p21^{waf1/cip1}$ expression, one of the well-known regulators of the cell cycle. We found that 10 μM (*S*)-**1** treatment for 48 hs induced higher expression of the protein in HT-29 cells compared to (*R*)-**1** and (*R*,*S*)-**2**, whereas treatment with all three compounds slightly affected $p21^{waf1/cip1}$ expression in HEK293T cells (Figure 6B). The above described results indicate that the colon cancer derived cell line HT-29 appears to be more susceptible to (*S*)-**1** than normal HEK293T cells, considered as normal, thus implying the possibility of future experimentations for these compounds in preclinical and clinical trials.

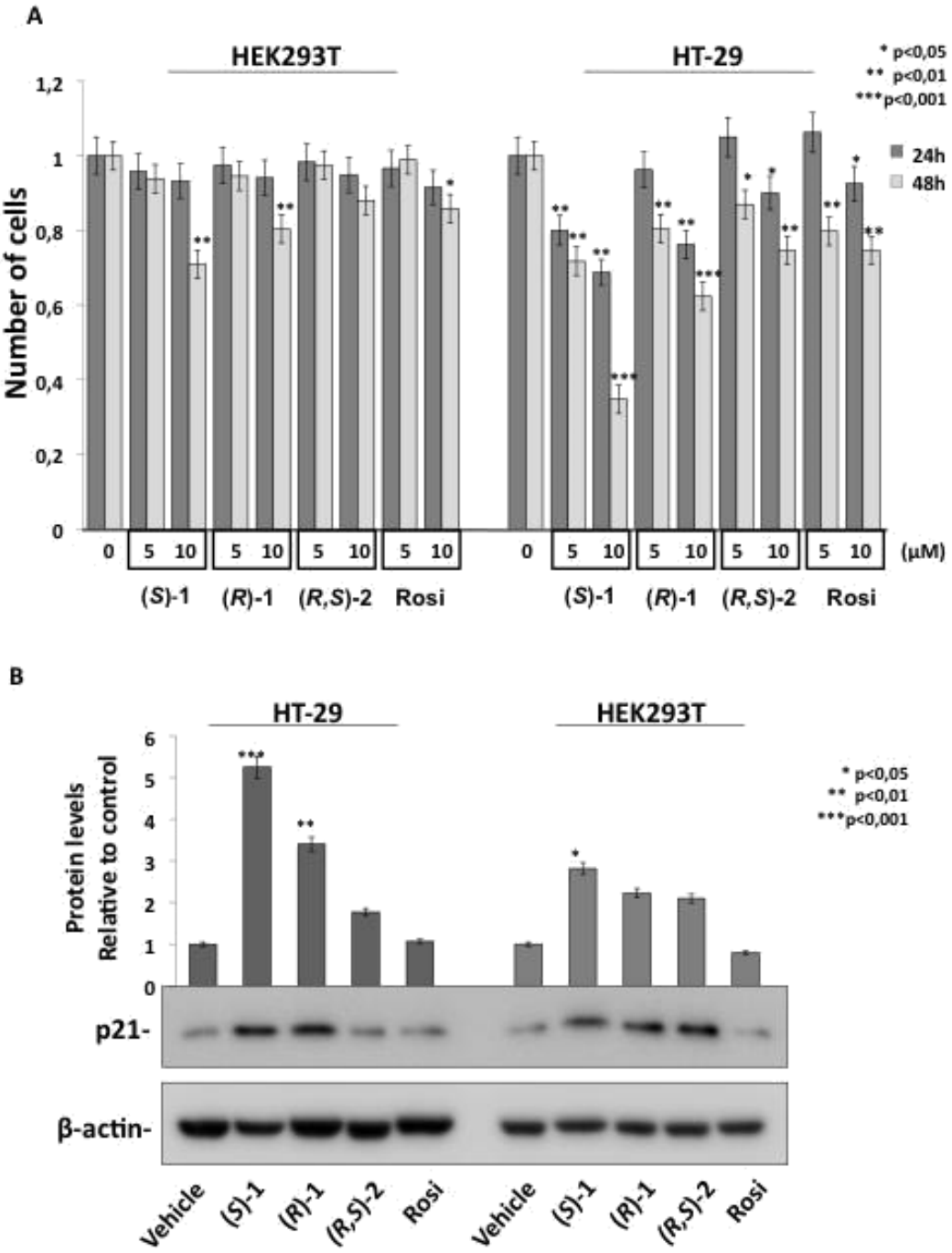

Figure 6. (A) Evaluation of the antiproliferative potential of (*S*)-**1**, (*R*)-**1** and (*R,S*)-**2** in human embryonic kidney HEK293T and colon cancer HT-29 cells. To assess the effect of the different compounds, exponentially growing HEK293T and HT-29 cells were exposed or not to 5 and 10 μM of each drug for 24 and 48 hs, collected and counted. The data shown here are the mean ± SD of three independent experiments performed in duplicate. Results were similar in three independent experiments. * $p < 0.05$, ** $p < 0.01$, *** $p < 0.001$, respectively, when compared to vehicle treated cells. (B) Total protein extracts from HT-29 and HEK293T cells untreated or treated with 10 μM (*S*)-**1**, (*R*)-**1** and (*R,S*)-**2** for 48 hs were analysed by Western blot with an anti-$p21^{waf1/cip1}$ antibody. An anti-β-actin antibody was used as a loading control. The bar graphs represent the mean ± SD of p21/β-actin of at least three independent experiments. The Western blotting assays reported here are representative of a single experiment.

6. Compounds (*S*)-1, (*R*)-1 and (*R,S*)-2 interfere with the β-catenin/TCF pathway and determine cell proliferation arrest

The strong cell growth inhibition exhibited by (*S*)-**1** associated with the weak transactivation potential prompted us to investigate whether this compound might activate antiproliferative pathways that are not or are only partially activated by classical PPARγ full agonists. The Wnt/β-catenin signalling is overexpressed in the majority of colorectal cancers and its dysregulation is one of the leading causes of such a malignancy.[51] We assessed the ability of our compounds to activate this pathway in HEK293T cells in which the Wnt/β-catenin pathway is not active and can be induced upon exposure to selected stimuli such as lithium chloride (LiCl).[52] Cells were transiently transfected with the Top-FLASH reporter plasmid carrying the luciferase gene under the control of multiple β-catenin responsive elements, a well-accepted system to assess activation of this pathway. LiCl administration produced high luciferase activity that was set at 100% in our assays (Figure 7). A combination of LiCl and rosiglitazone resulted in about 50% reduction of luciferase activity; the combination of LiCl with (*R*)-**1** or compound **2** produced similar effects (about 50% reduction) while a slightly further decrease was observed with (*S*)-**1** (about 40% reduction)**.**

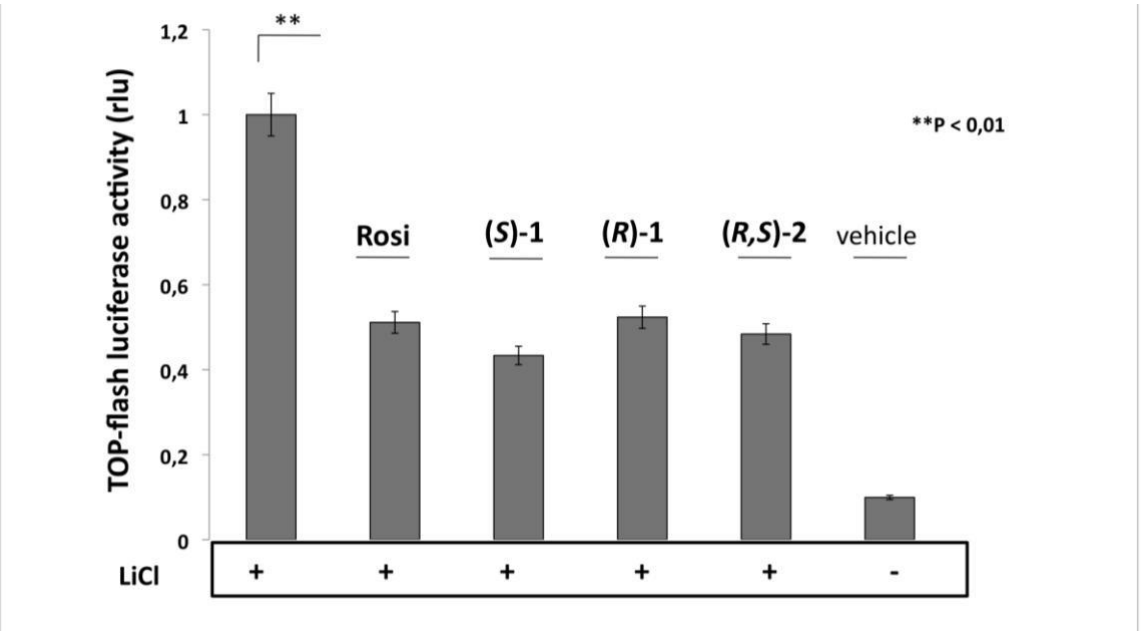

Figure 7. Top-FLASH assay in HEK293T cells. Cells were transfected with the Top-FLASH reporter plasmid and, subsequently, exposed to 20 mM LiCl alone or in combination with 1 μM (*S*)-**1**, (*R*)-**1**, (*R*,*S*)-**2** or rosiglitazone for 24 hs. Luciferase reporter gene activity was determined 48 hs after transfection by a specific assay. The results of the transfections are reported as luciferase fold induction after normalization to β-galactosidase activity used as control of transfection efficiency. Data shown are mean ± SD of three independent experiments performed in duplicate.

To further prove the specificity of these effects, we treated HT-29 cells with the various compounds and assessed the levels of c-Myc and cyclin D1, two β-catenin target proteins. We selected this cell line as it bears a mutation in the APC gene and thus the Wnt/β-catenin pathway is already activated;[53] accordingly, c-Myc and cyclin D1 are already elevated in basal conditions. Treatment with rosiglitazone diminished the levels of both proteins; exposure to (*S*)-**1**, (*R*)-**1** and (*R*,*S*)-**2** resulted in a similar reduction for cyclin D1, more evident for c-Myc (Figure 8). Interestingly, (*S*)-**1** displayed a stronger effect on both proteins, in line with the results of the transactivation assay reported above.

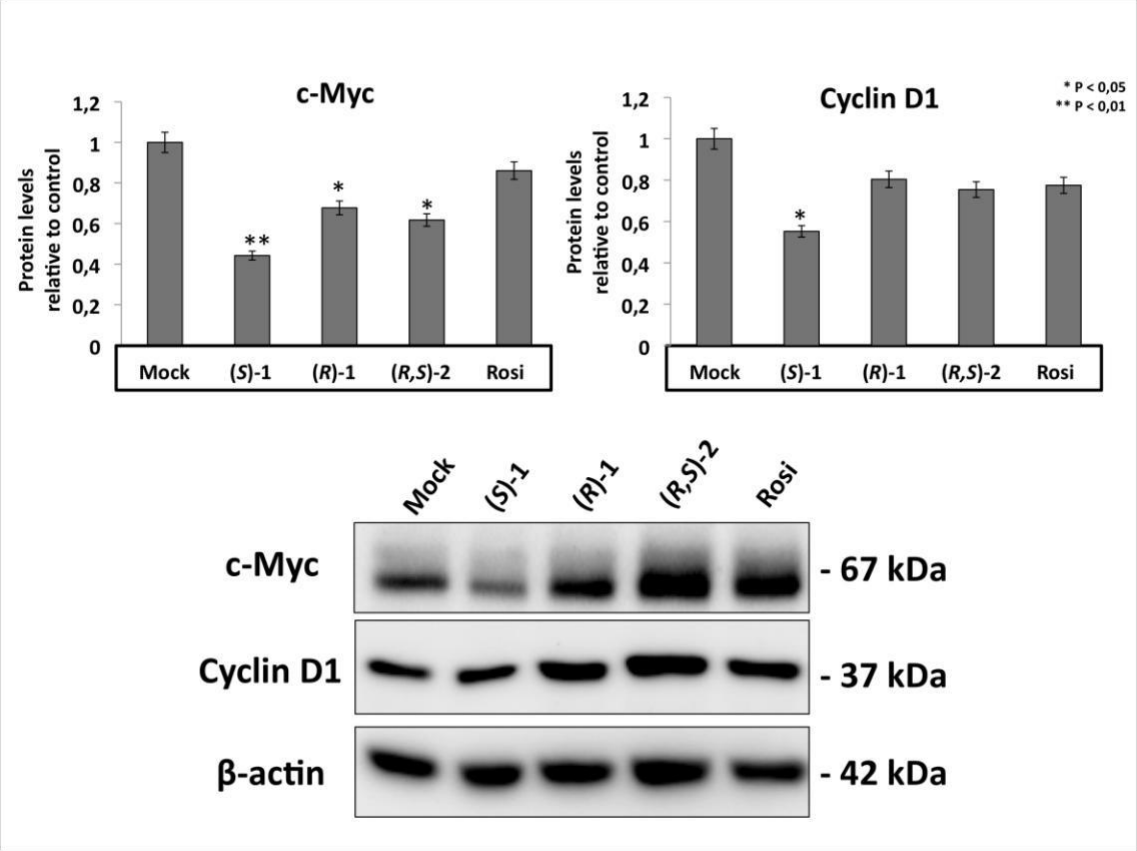

Figure 8. (*S*)-**1**, (*R*)-**1** and (*R,S*)-**2** interfere with the Wnt/β-catenin pathway. Total protein extracts from HT-29 cells untreated or treated with 10 μM of each of the compounds (*S*)-**1**, (*R*)-**1** and (*R,S*)-**2** or Rosiglitazone for 24 hs were analyzed by Western blot for c-Myc and cyclin D1 expression. β-actin was used as loading control. The bar graphs represent the mean ± SD of proteins/β-actin of at least three independent experiments. The results reported here are representative of a single Western blot experiment.

7. Effects of (*R*)-1, (*S*)-1 and (*R,S*)-2 on the carnitine shuttle system and mitochondrial functions.

Fatty acids oxidation takes place in mitochondria and is coupled to oxidative phosphorylation for energy production. In order to be degraded, fatty acids are transported from the cytosol by means of the carnitine shuttle system: once activated to acyl-CoAs, they are transferred to carnitine by the carnitine-palmitoyl-transferase 1 (CPT1), located on the surface of the outer mitochondrial membrane;[54,55] the acylcarnitine crosses the outer membrane [56] and translocates through the inner mitochondrial membrane by virtue of the carnitine/acylcarnitine carrier (CAC). Therefore, the carnitine shuttle system is essential for the mitochondrial oxidation of fatty acids.[57] It has been demonstrated that two fibrates (Wy-14,643 and GW7647) stimulate CAC transcript and protein levels in primary and secondary cell lines as they act as PPARα ligands, providing a molecular explanation of their hypolipidemic action.[36] Based on these premises, we evaluated whether our fibrate-like drugs could upregulate mitochondrial CAC and CPT1 gene expression by treating HepG2 cells with 1 μM of (*R*)-**1**, (*S*)-**1** or (*R,S*)-**2** for 24 hs; Wy-14,643 (50 μM) was used as reference compound. Both CAC and CPT1 mRNA levels displayed a significant increase in treated HepG2 when compared to control cells by real-time PCR (Figure 9A,B). This was mirrored by a parallel increase of the corresponding proteins that was more evident for CPT1 (Figure 9C,D). These effects turned out to be similar or even greater than those observed for Wy-14,643, whose concentration to activate both genes was fifty-fold higher (50 vs 1 μM).

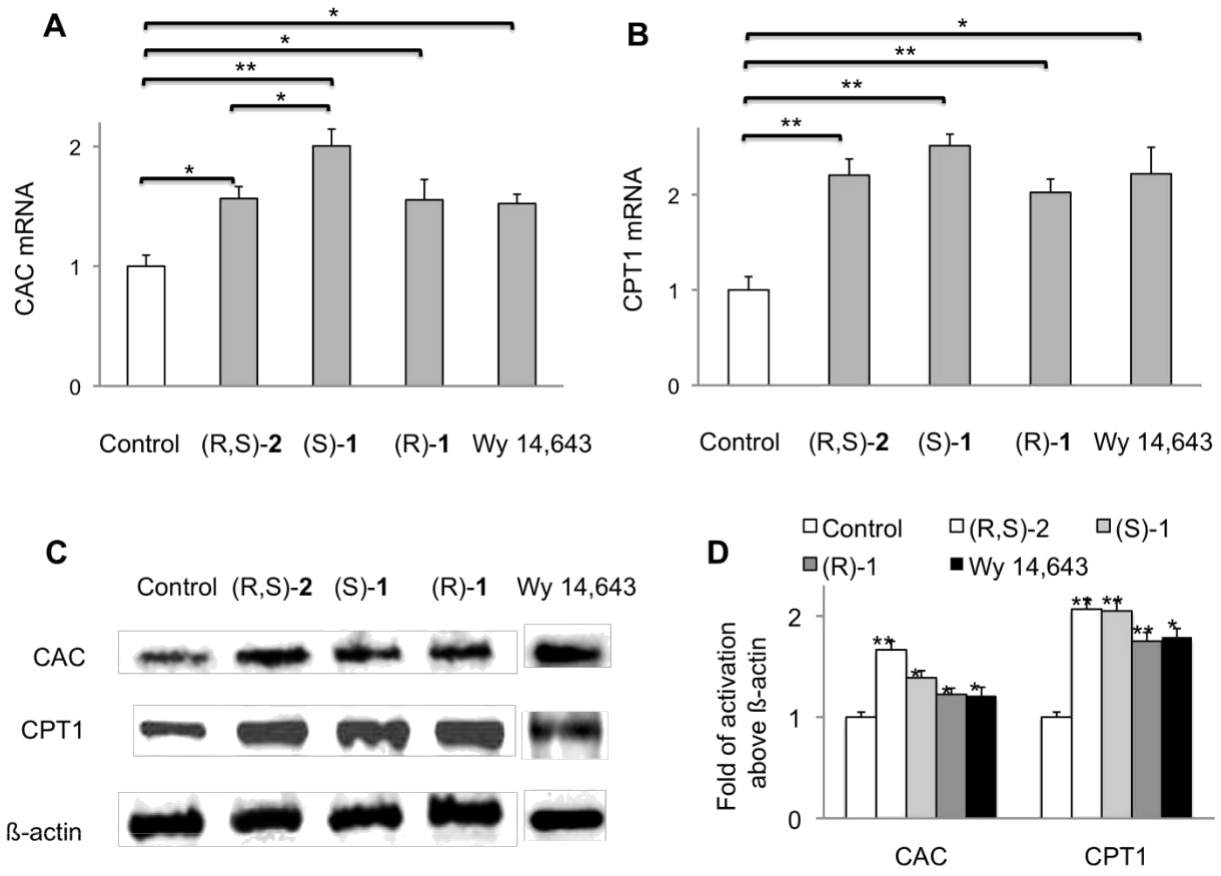

Figure 9. Effect of (*R*)-**1**, (*S*)-**1** and (*R,S*)-**2** on CAC and CPT1 gene expression. Total RNA extracted from HepG2 cells, untreated or treated with 1 μM (*R*)-**1**, 1 μM (*S*)-**1** or 1 μM (*R,S*)-**2** or 50 μM Wy-14,643 for 24 hs, was used to quantify A) CAC mRNA and B) CPT1 mRNA by real-time PCR; data are the mean ± SD of three independent duplicate experiments. C) Total protein extracts from HepG2 cells, untreated or treated for 48 hs as described in panels and B), were immunoblotted for CAC, CPT1 and β-actin using specific antibodies. D) The intensities of immunolabeled protein bands as in panel C) were quantified by densitometric scanning and quantification is expressed as fold-change of CAC and CPT1 protein signals relative to control cells. In A) and B), data are means ± SD from three independent experiments (*p<0.05, **p<0.01; one-way ANOVA, Bonferroni test). Western blot data in C) are representative of three independent experiments with similar results.

We also tested whether our compounds could activate PPARα transcription in a positive regulatory loop, as a PPRE (peroxisome proliferator-activated receptor response element) is present in the human PPARα promoter.[58,59] To this end, HepG2 cells were incubated with each compound and Wy-14,643 as control and PPARα mRNA and protein levels assessed. All of our compounds, as well as Wy-14,643, increased PPARα mRNA and protein levels (Figure 10A,B). Also in this case, the Wy-14,643 concentration was fifty-fold higher than (*R*)-**1**, (*S*)-**1** and (*R,S*)-**2**.

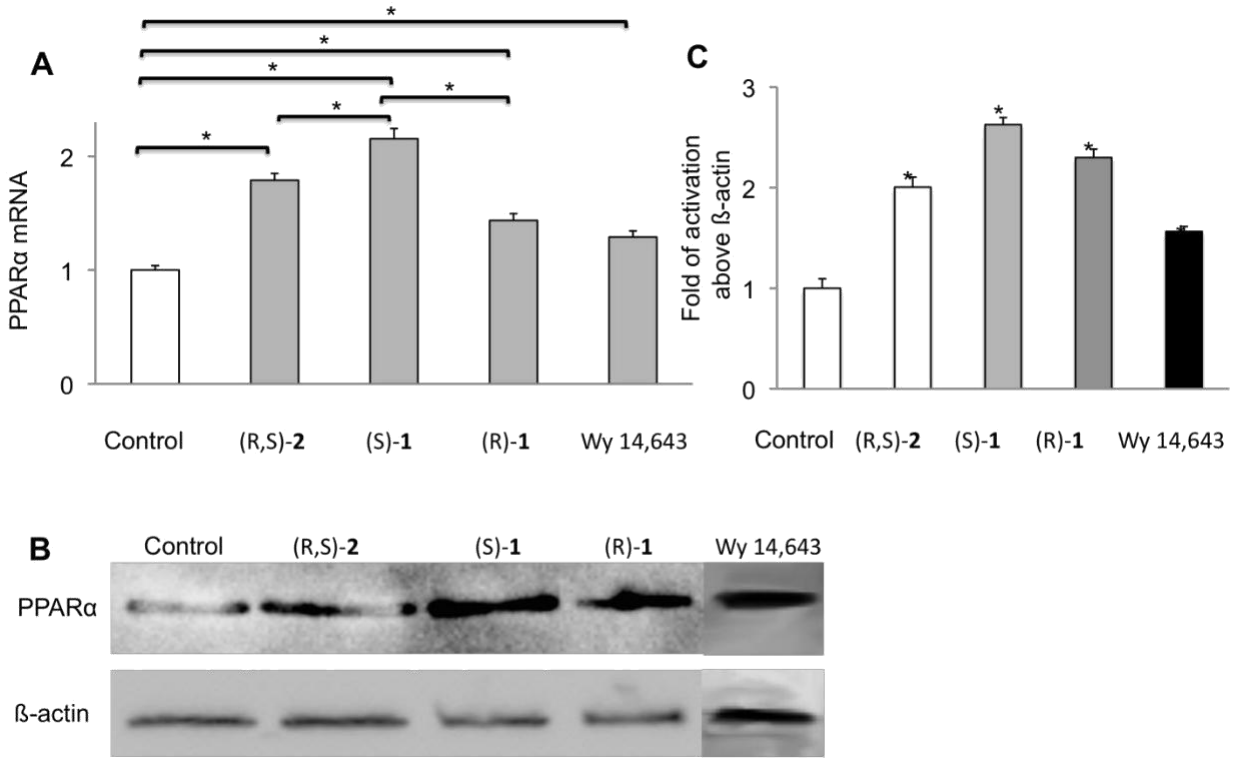

Figure 10. PPARα gene expression in (*R*)-**1**, (*S*)-**1** and (*R,S*)-**2** treated cells. A) Total RNA extracted from HepG2 cells untreated or treated with 1 μM (*R*)-**1**, 1 μM (*S*)-**1**, 1 μM (*R,S*)-**2** or 50 μM Wy-14,643 for 24 hs, was used to quantify PPARα mRNA by real-time PCR; data are the mean ± SD of three independent duplicate experiments. B) Total protein extracts from HepG2 cells, untreated or treated for 48 hs as in A), were immunoblotted for PPARα and β-actin using specific antibodies. C) The intensities of immunolabeled protein bands as in panel B) were quantified by densitometric scanning and quantification is expressed as fold-change of PPARα protein signals relative to control cells. In A), data are means ± SD from three independent experiments (*$p<0.05$; one-way ANOVA, Bonferroni test). Western blot data in B) are representative of three independent experiments with similar results.

It is known that mitochondrial dysfunction is linked to dyslipidemia and hypercholesterolemia [60] and impaired mitochondrial biogenesis is observed in these pathological conditions.[61] In addition, numerous studies in humans and animal models have shown that insulin resistance is frequently associated with reduced mitochondrial mass or oxidative function in insulin sensitive tissues, leading to the hypothesis that defective overall mitochondrial activity could play a relevant role in the etiology of insulin resistance and, hence, in type 2 diabetes. The possibility of increasing the mitochondrial mass and oxidative activity is, then, viewed as a potential therapeutic approach for the treatment of insulin resistance.[62] For this reason, we evaluated the effect of (*R*)-**1**, (*S*)-**1**, (*R,S*)-**2**, and Wy-14,643 on the mitochondrial mass in HepG2 cells transduced with CellLight®

Mitochondria-GFP BacMam 2.0, treated for twenty-four hours with each fibrate-like drug and analyzed under a fluorescent microscope or by a microplate reader. All compounds increased the mitochondrial mass by 30% as proven by a more intense fluorescent signal than control cells (Figure 11A,B). Also in this case, Wy-14,643, the positive control, produced the same effect but at a fifty-fold higher concentration. Collectively, these findings show that all tested compounds significantly induce carnitine shuttle genes as direct targets of PPARα, the master regulator of mitochondrial fatty acid β-oxidation.

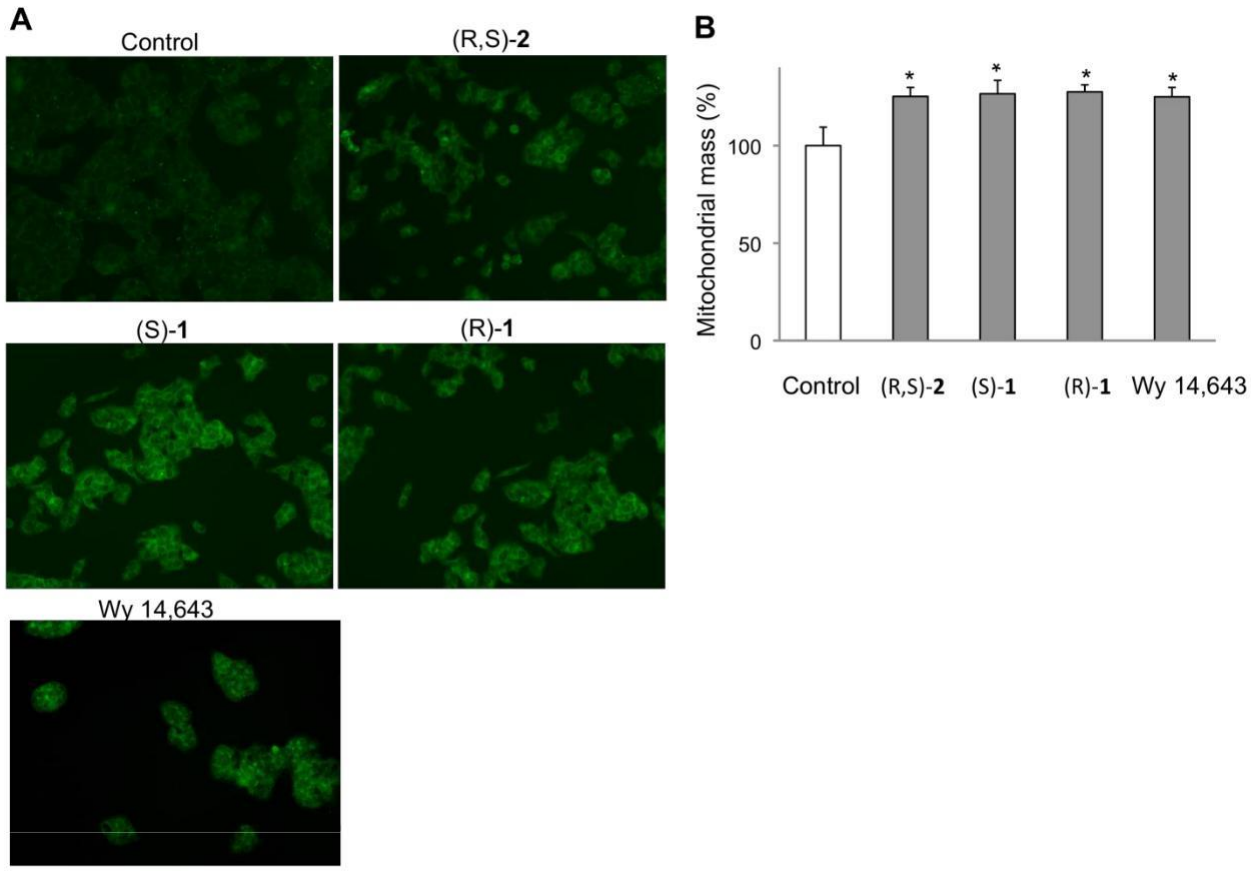

Figure 11. Changes in mitochondrial mass after (*R*)-**1**, (*S*)-**1** and (*R*,*S*)-**2** treatment. A) HepG2 cells treated with CellLight® Mitochondria-GFP BacMam 2.0 in the presence or absence (control) of 1 μM (*R*)-**1**, 1 μM (*S*)-**1**, 1 μM (*R*,*S*)-**2** or 50 μM Wy-14,643 were observed (magnification 20x). B) HepG2 cells were treated as in A) and the fluorescence of cell extracts was measured by using a microplate reader at 475 nm for excitation and 500-550 nm for emission. Data are means ± SD from three independent experiments (*$p<0.05$; one-way ANOVA, Bonferroni test). Images showed in (A) are representative of three independent experiments with similar results.

PPARα itself is upregulated by these compounds that exhibit also the ability to enhance mitochondrial biogenesis. Indeed, PPARα activation has been shown to be sufficient to drive mitochondrial biogenesis in pathological conditions,[63] as it activates PGC-1α and other transcription factors gene expression to coordinate mitochondrial biogenesis. These events, most probably, lead to an adaptive response that results in an increased mitochondrial function and fatty acid β-oxidation. Our results clearly demonstrate that (*R*)-**1**, (*S*)-**1** and (*R*,*S*)-**2** can activate carnitine shuttle system through upregulation of CAC, CPT1 and PPARα genes and induce a significant mitochondrial biogenesis that in turn sustains fatty acid β-oxidation.

8. Conclusion

In the present study, we investigated the properties of a short series of compounds characterized by the presence of the diphenylmethane skeleton that has already shown its usefulness as a multi-template for nuclear receptors. We provide evidence that some of these compounds act as potent dual PPARα/γ partial agonists as documented by docking experiments performed to understand the molecular basis of their partial agonism and the lack of stereoselectivity between the enantiomers of the most active compound **1**. We also show that both enantiomers of **1** and racemic **2** have the ability to inhibit cellular proliferation in colon cancer cell lines due, at least in part, to a downregulation of the Wnt/β-catenin signalling which is mutated and upregulated in the majority of colorectal cancers. Among the three compounds investigated, (*R*)-**1**, (*S*)-**1**, and (*R*,*S*)-**2**, the stereoisomer (*S*)-**1** seems to display a stronger antiproliferative effect and increased inhibition of the Wnt/β-catenin signalling. We also demonstrate that (*R*)-**1**, (*S*)-**1** and (*R*,*S*)-**2** are able to activate the carnitine shuttle system through upregulation of carnitine/acylcarnitine carrier (CAC), carnitine-palmitoyl-transferase 1 (CPT1) and PPARα genes essential for the mitochondrial fatty acids β-oxidation. Moreover, these

compounds induce a significant mitochondrial biogenesis, an effect which is currently viewed as a potential therapeutic approach for the treatment of dyslipidemia, hypercholesterolemia and insulin resistance, pathological conditions frequently associated with reduced mitochondrial mass or oxidative function in insulin sensitive tissues. Collectively, (*R*)-**1**, (*S*)-**1** and (*R,S*)-**2** are dual PPARα/γ ligands with promising biological effects in cellular systems and thus could stand as leads for the development of new molecules for the treatment of dyslipidemic type 2 diabetes and/or cancer. The lack of any activity toward FXR, though the high similarity with some recent phenoxyacetic acids reported in the literature as FXR agonists, indicates that this receptor is much more selective than PPARs and even small modifications in the chemical structure of an agonist can produce inactive molecules. However, even though only a few drugs are reported as dual PPAR/FXR agonists, the challenge to identify this type of ligands is still open and, with this aim, a fine-tuned search for new analogs of compounds **1** and **2** is now in progress.

9. Experimental section

9.1 Chemical Methods

Column chromatography was performed on ICN silica gel 60Å (63-200 μm) as a stationary phase. Melting points were determined in open capillaries on a Gallenkamp electrothermal apparatus and are uncorrected. Mass spectra were recorded on an HP GC/MS 6890-5973 MSD spectrometer, electron impact 70 eV, equipped with HP chemstation or an Agilent LC/MS 1100 Series LC/MSD Trap System VL spectrometer, electrospray ionization (ESI). HR-MS analyses were carried out using an electrospray interface and a Q-TOF mass spectrometer (Agilent 6530 Accurate Mass Q-TOF LC/MS, Palo Alto, CA). Ionization was achieved in the negative ion mode. ^{1}H-NMR and ^{13}C-NMR spectra were recorded in $CDCl_3$ (the use of other solvents is specified) on a Varian-Mercury 300 (300 MHz) or an Agilent 500 (500 MHz) spectrometer. Chemical shifts are expressed as parts per million (ppm, δ). Microanalyses of solid compounds were carried out with an Eurovector Euro EA 3000 model analyzer and were within ±0.4% of the theoretical values. Optical rotations were measured with a Perkin-Elmer 341 polarimeter at room temperature (20 °C): concentrations are expressed as g/100 mL. The enantiomeric excesses of acids were determined by HPLC analysis on a Chiralcel OD column (4.6 mm i.d. x 250 mm, Daicel Chemical Industries, Ltd., Tokyo, Japan). Analytical liquid chromatography was performed on a PE chromatograph equipped with a Rheodyne 7725i model injector, a 785A model UV/Vis detector, a series 200 model pump and NCI 900 model interface. Chemicals were from Sigma-Aldrich (Milan, Italy) and were used without any further purification.

*9.2 Preparation of 4-(chloromethyl)-2-phenyl-1,3-oxazole (**7**) and 4-(chloromethyl)-2-(2,6-dichlorophenyl)-1,3-oxazole (**8**). General procedure*

A mixture of the appropriate benzamide (0.0083 mol) and 1,3-dichloroacetone (0.0099 mol) was warmed in a sealed vial at 180 °C for 2 h. The resulting solution was cooled at room temperature, added with CH_2Cl_2 and washed with H_2O (2x25 mL). The organic layer was dried over Na_2SO_4 and

filtered off. Then the solvent was evaporated in vacuo to give a brown oil which was chromatographed on a silica gel column (*n*-hexane/ethyl acetate 95:5 as eluent) affording the desired compound as a white solid.

*9.2.1. 4-(Chloromethyl)-2-phenyl-1,3-oxazole (**7**)*

51% Yield; mp = 54-55 °C; GC/MS, *m/z* (%): 195 (M^++2, 16), 193 (M^+, 48), 158 ($C_{10}H_8NO^+$, 88), 103 ($C_7H_5N^+$, 100); ^{1}H-NMR: 4.58 (s, 2H, CH_2), 7.44-7.47 and 8.03-8.06 (m, 5H, aromatics), 7.71 (s, 1H, CH).

*9.2.2. 4-(Chloromethyl)-2-(2,6-dichlorophenyl)-1,3-oxazole (**8**)*

6% Yield; GC/MS, *m/z* (%): 265 (M^++4, 12), 263 (M^++2, 37), 261 (M^+, 38), 226 ($C_{10}H_6Cl_2NO^+$, 100); ^{1}H-NMR: 4.63 (s, 2H, CH_2), 7.38-7.42 (m, 3H, aromatics), 7.83 (s, 1H, CH).

*9.3 Preparation of 4-(chloromethyl)-5-methyl-2-phenyl-1,3-oxazole (**9**) and 4-(chloromethyl)-2-(2,6-dichlorophenyl)-5-methyl-2-phenyl-1,3-oxazole (**10**). General procedure*

A mixture of butan-2,3-dione (5 mL), $NH_2OH{\cdot}HCl$ (3.97 g; 0.058 mol) and CH_3COONa (9.52 g; 0.116 mol) was dissolved in H_2O/EtOH 96% (1:5, 250 mL) at 0 °C and stirred at room temperature for 4 h. Then ethanol was distilled off, and the residue was added with water and extracted with CH_2Cl_2. The organic layer was dried over Na_2SO_4 and filtered. The solvent was evaporated in vacuo to give *butane-2,3-dione oxime* as a pale yellow solid (3.96 g; 0.039 mol): 68% yield;

GC/MS, *m/z* (%): 101 (M^+, 29), 58 ($C_2H_4NO^+$, 7), 43 ($C_2H_3O^+$, 100); ^{1}H-NMR: 1.86 (s, 3H, CH_3-C=O), 2.26 (s, 3H, CH_3-C=N), 11.27 (s, 1H, OH). The so obtained oxime (1.40 g; 0.014 mol) and the appropriate benzaldheyde (0.015 mol) were dissolved in a mixture of 4M HCl/dioxane (1:1, 20 mL) and stirred at room temperature. After 4 h the solution was cooled to 0 °C and the resulting precipitate was filtered off, suspended into H_2O and NH_4OH (pH=8) and extracted with $CHCl_3$ (3x30 mL). The organic layer was dried over Na_2SO_4 and filtered. The solvent was evaporated in

vacuo to give the corresponding N-oxides as pale yellow solids. *4,5-Dimethyl-2-phenyl-1,3-oxazole 3-oxide*. 35% Yield; ^{1}H-NMR: 2.23 and 2.37 (2 s, 6H, 2 CH_3), 7.44-7.53 and 8.43-8.47 (m, 5H, aromatics). *2-(2,6-Dichlorophenyl)-4,5-dimethyl-1,3-oxazole 3-oxide*. 18% yield; ^{1}H-NMR: 2.35 and 2.48 (2 s, 6H, 2 CH_3); 7.20-7.32 (m, 3H, aromatics). $POCl_3$ (0.802 g; 0.052 mmol) in anhydrous $CHCl_3$ (15 mL) was added dropwise to a solution of the N-oxide (0.049 mol) in anhydrous $CHCl_3$ (15 mL) at 0 °C. The resulting mixture was refluxed for 8 h under nitrogen atmosphere, then cooled and treated with H_2O and NH_4OH (pH=8). The two layers were separated and the aqueous phase was extracted with $CHCl_3$ (2x30 mL). The organic layers were collected, washed with brine (2x50 mL), dried over Na_2SO_4 and filtered off. The solvent was evaporated in vacuo to give a brown solid residue which was chromatographed on a silica gel column (*n*-hexane/ethyl acetate 80:20 as eluent) affording the desired compounds as pale yellow solids.

*9.3.1. 4-(Chloromethyl)-5-methyl-2-phenyl-1,3-oxazole (**9**)*

53% Yield; mp = 83-84 °C; GC/MS, *m/z* (%): 209 (M^++2, 12), 207 (M^+, 38), 172 ($C_{11}H_{10}NO^+$, 100), 77 ($C_6H_5^+$, 10); ^{1}H-NMR: 2.43 (s, 3H, CH_3), 4.56 (s, 2H, CH_2), 7.42-7.46 and 7.98-8.02 (m, 5H, aromatics).

*9.3.2. 4-(Chloromethyl)-2-(2,6-dichlorophenyl)-5-methyl-2-phenyl-1,3-oxazole (**10**)*

18% Yield; GC/MS, *m/z* (%): 279 (M^++4, 9), 277 (M^++2, 27), 275 (M^+, 27), 240 ($C_{11}H_8Cl_2NO^+$, 100); ^{1}H-NMR: 2.45 (s, 3H, CH_3), 4.59 (s, 2H, CH_2), 7.35-7.42 (m, 3H, aromatics).

*9.4. Preparation of 4-[1-ethyl-1-(4-hydroxyphenyl)propyl]phenol (**11**)*

Phenol (0.106 mol), 3-pentanone (3.5 mL) and methansulfonic acid (2.6 mL) were stirred at room temperature for 5 days. Then, the mixture was dissolved in EtOAc and washed (3x30 mL) with brine, dried over Na_2SO_4 and evaporated to dryness affording a white solid which was crystallized from $CHCl_3$/*n*-hexane. 34% Yield; mp: 85-86 °C; GC/MS, *m/z* (%): 256 (M^+, 5), 227 ($C_{15}H_{15}O_2^+$,

100), 212 ($C_{14}H_{12}O_2^+$, 3), 133 ($C_9H_9O^+$, 14); ^{1}H NMR: 0.60 (t, J=7.42, 6H, 2 CH_3), 2.01 (q, J=7.42, 4H, 2 CH_2), 4.60 (bs, 2H, 2 OH, D_2O exchanged), 6.70-6.74 and 7.00-7.04 (m, 8H, aromatics).

*9.5. Preparation of 2-[4-(4-hydroxybenzyl)phenoxy]propionic acid methyl ester (**12**) and 2-{4-[1-ethyl-1-(4-hydroxyphenyl)propyl]phenoxy}propionic acid ethyl ester (**13**). General procedure*

A suspension of NaH (0.009 mol) in anhydrous THF (20 mL) was cooled to 0 °C and added with a solution of commercially available bis(4-hydroxyphenyl)methane or **11** (0.009 mol) in anhydrous THF (15 mL). After 30 minutes, a solution of methyl or ethyl 2-bromopropionate (0.009 mol) in anhydrous THF (15 mL) was added dropwise and the mixture warmed at 60 °C for 96 h. The solvent was evaporated and the residue was added with ice and extracted with ethyl acetate. The organic layer was washed with 2 N HCl and twice with brine, dried over Na_2SO_4, filtered and evaporated to dryness. The solid residue was chromatographed on a silica gel column (*n*-hexane/ethyl acetate 85:15 as eluent) affording the desired compounds as colorless oils.

*9.5.1. 2-[4-(4-Hydroxybenzyl)phenoxy]propionic acid methyl ester (**12**)*

36% Yield; GC/MS, *m/z* (%): 286 (M^+, 100), 227 ($C_{15}H_{15}O_2^+$, 64), 199 ($C_{13}H_{11}O_2^+$, 62), 107 ($C_7H_7O^+$, 54); ^{1}H-NMR: 1.60 (d, J=6.88, 3H, CH-C*H*$_3$), 3.75 (s, 3H, $COOCH_3$), 3.83 (s, 2H, CH_2), 4.72 (q + bs, J=6.88, 2H, CH_3-C*H* + OH, D_2O exchanged), 6.73-6.80 (m, 4H, aromatics), 7.00-7.07 (m, 4H, aromatics).

*9.5.2. 2-{4-[1-Ethyl-1-(4-hydroxyphenyl)propyl]phenoxy}propionic acid ethyl ester (**13**)*

18% Yield; GC/MS, *m/z* (%): 356 (M^+, 4), 327 ($C_{20}H_{23}O_4^+$, 100); ^{1}H-NMR: 0.58 (t, J=7.42, 6H, 2 C*H*$_3$-CH_2), 1.23 (t, J=7.15, 3H, C*H*$_3$-CH_2-O), 1.58 (d, J=6.88, 3H, C*H*$_3$-CH), 2.01 (q, J=7.42, 4H, 2 C*H*$_2$$CH_3$), 4.17-4.26 (m, 2H, OC*H*$_2$-CH_3), 4.72 (q + bs, J=6.88, 2H, CH_3-C*H* + OH, D_2O exchanged) 6.68-6.77 and 6.98-7.02 (m, 8H, aromatics).

*9.6. Preparation of the methyl esters (R)-**12** and (S)-**12**. General procedure*

To an ice-bath cooled mixture of (*R*)-or (*S*)-methyl lactate (4.8 mmol), bis(4-hydroxyphenyl)methane (4.8 mmol), and triphenylphosphine (4.8 mmol) in anhydrous THF (30 mL), a solution of diisopropyl azodicarboxylate (DIAD, 4.8 mmol) in anhydrous THF (20 mL) was added dropwise under nitrogen atmosphere. The mixture was allowed to warm to room temperature and stirred for overnight. The solvent was evaporated affording an oil which was chromatographed on a silica gel column (*n*-hexane/ethyl acetate 9:1 as eluent) to give the target methyl esters as white solids.

*9.6.1. (R)-2-[4-(4-Hydroxybenzyl)phenoxy]propionic acid methyl ester, (R)-**12**. 37% Yield.*

*9.6.2. (S)-2-[4-(4-Hydroxybenzyl)phenoxy]propionic acid methyl ester, (S)-**12**. 30% Yield.*

*9.7. Preparation of the esters **14-19**. General Procedure*

Cs_2CO_3 (3 mmol) was added to a stirred solution of **12** or **13** (1 mmol) in acetonitrile (10 mL). After 0.5 h, a solution of the suitable 4-chloromethyl-1,3-oxazole **7-10** (1.5 mmol) in acetonitrile (10 mL) was added dropwise and the resulting mixture was refluxed for 4 h. Then, acetonitrile was evaporated and the residue was taken up with ethyl acetate. The organic phase was washed with 0.5 N NaOH and brine, dried over Na_2SO_4 and evaporated to dryness affording yellows oils, which were chromatographed on a silica gel column (*n*-hexane/ethyl acetate 95:5 as eluent) affording the desired compounds as colourless oils.

*9.7.1. 2-{4-[4-(2-Phenyl-1,3-oxazol-4-ylmethoxy)benzyl]phenoxy}propionic acid methyl ester (**14**)*

90% Yield; GC/MS, *m/z* (%): 443 (M^+, 18), 158 ($C_{10}H_8NO^+$, 100), 103 ($C_7H_5N^+$, 49); ^{1}H-NMR (DMSO-d_6): 1.45 (d, J=6.88, 3H, C*H*$_3$-CH), 3.64 (s, 3H, CH_3-O), 3.78 (s, 2H, CH_2-Ph), 4.88 (q, J=6.88, 1H, C*H*-CH_3), 4.99 (s, 2H, CH_2-O), 6.77-7.12 (m, 8H, aromatics), 7.51-7.97 (m, 5H, aromatics), 8.27 (s, 1H, CH-C=C-N).

*9.7.2. 2-{4-[4-(5-Methyl-2-phenyl-1,3-oxazol-4-ylmethoxy)benzyl]phenoxy}propionic acid methyl ester (**15**)*

67% Yield; GC/MS, *m/z* (%): 457 (M^+, 4), 172 ($C_{11}H_{10}NO^+$, 100); ^{1}H-NMR (DMSO-d_6): 1.45 (d, J=6.87, 3H, C*H*$_3$-CH), 2.41 (s, 3H, CH_3-C=C-N), 3.63 (s, 3H, CH_3-O), 3.78 (s, 2H, CH_2-Ph); 4.86 (q, J=6.87, 1H, C*H*-CH_3); 4.93 (s, 2H, CH_2-O); 6.74-7.93 (m, 13H aromatics).

*9.7.3. 2-{4-{1-Ethyl-1-[4-(2-phenyl-1,3-oxazol-4-ylmethoxy)phenyl]propyl}phenoxy}propionic acid ethyl ester (**16**)*

51% Yield; GC/MS, *m/z* (%): 513 (M^+, 2), 484 ($C_{32}H_{35}NO_5^+$, 93), 158 ($C_{10}H_8NO^+$, 100); ^{1}H-NMR (DMSO-d_6): 0.59 (t, J=7.16, 6H, 2 C*H*$_3$-CH_2), 0.85 (t, J=7.15, 3H, C*H*$_3$-CH_2-O), 1.23 (d, J=6.88, 3H, C*H*$_3$-CH); 2.02 (q, J=7.16, 4H, 2 C*H*$_2$-CH_3), 4.20 (q, J=7.15, 2H, O-C*H*$_2$-CH_3), 4.68 (q, J=6.88, 1H, C*H*-CH_3), 5.09 (s, 2H, CH_2-O); 6.69-7.09, 7.45-7.49 and 7.98-8.13 (m, 13H, aromatics), 7.74 (s, 1H, O-CH=C).

*9.7.4. 2-{4-{1-Ethyl-1-[4-(5-methyl-2-phenyl-1,3-oxazol-4ylmethoxy)phenyl]propyl}phenoxy}propionic acid ethyl ester (**17**)*

88% Yield; GC/MS, *m/z* (%): 527 ($C_{33}H_{37}NO_5^+$, 2), 498 ($C_{31}H_{32}NO_5^+$, 13), 327 ($C_{22}H_{27}O_4^+$, 35), 172 ($C_{11}H_{10}NO^+$, 100); ^{1}H-NMR: 0.59 (t, J=7.42, 6H, 2 *CH*$_3$-CH_2), 1.23 (t, J=7.15, 3H, *CH*$_3$-CH_2-O), 1.59 (d, J=6.60, 3H, *CH*$_3$-CH), 2.04 (q, J=7.42, 4H, 2 *CH*$_2$-CH_3), 2.46 (s, 3H, CH_3-C=C-N), 4.19 (q, J=7.15, 2H, O-*CH*$_2$-CH_3), 4.70 (q, J=6.60, 1H, *CH*-CH_3), 5.04 (s, 2H, CH_2-O), 6.74-7.49 (m, 13H, aromatics).

*9.7.5. 2-{4-{1-{4-[2-(2,6-Dichloro-phenyl)-1,3-oxazol-4-ylmethoxy]phenyl}-1-ethyl-propyl}-phenoxy}propionic acid ethyl ester (**18**)*

52% Yield; ESI-MS, *m/z* (%): 608 (M^++27, 13), 606 (M^++25, 66), 604 (M^++23, 100), 551 ($C_{30}H_{27}Cl_2NO_3^+$,13); ^{1}H-NMR: 0.59 (t, , J=7.42, 6H, 2 CH_2C*H*$_3$), 1.23 (t, J=7.15, 3H, O-CH_2C*H*$_3$),

1.57 (d, J=6.88, 3H, CHC*H*$_3$), 2.02 (q, , J=7.42, 4H, 2 C*H*$_2$CH$_3$), 4.20 (m, 2H, O-C*H*$_2$CH$_3$), 4.70 (q, J=6.88, 1H, C*H*-CH$_3$), 5.11 (s, 2H, CH$_2$O), 6.73-7.42 (m, 11H, aromatics), 7.84 (s, 1H, O-CH=C).

*9.7.6. 2-{4-{1-{4-[2-(2,6-Dichloro-phenyl)-5-methyl-1,3-oxazol-4-ylmethoxy]phenyl}-1-ethyl-propyl}-phenoxy}propionic acid ethyl ester (**19**)*

48% Yield; ESI-MS, *m/z* (%): 622 (M^++27, 14), 620 (M^++25, 70), 618 (M^++23, 100), 551 ($C_{30}H_{27}Cl_2NO_3^+$,17); ^{1}H-NMR: 0.58 (t, J=7.43, 6H, 2 CH$_2$C*H*$_3$), 1.24 (t, J=7.15, 3H, O-CH$_2$C*H*$_3$), 1.58 (d, J=6.88, 3H, CHC*H*$_3$), 2.04 (q, J=7.43, 4H, 2 C*H*$_2$CH$_3$), 2.43 (s, 3H, CH$_3$-C=C-N), 4.21 (m, 2H, O-C*H*$_2$CH$_3$), 4.69 (q, J=6.88, 1H, C*H*-CH$_3$), 5.02 (s, 2H, CH$_2$O), 6.73-7.25 (m, 11H, aromatics).

*9.8. Preparation of the methyl esters (R)-**14** and (S)-**14***

For the preparation of these isomers the same procedure to obtain the racemate **14** was followed starting from (*R*)-**12** or (*S*)-**12**, respectively, and 1,3-oxazole **7**.

*9.8.1. (R)-2-{4-[4-(2-Phenyl-1,3-oxazol-4-ylmethoxy)benzyl]phenoxy}propionic acid methyl ester, (R)-**14.*** 83% Yield.

*9.8.2. (S)-2-{4-[4-(2-Phenyl-1,3-oxazol-4-ylmethoxy)benzyl]phenoxy}propionic acid methyl ester, (S)-**14**.* 74% Yield.

*9.9. Preparation of the final acids **1-6**. General Procedure*

A solution of the corresponding ethyl or methyl ester (5 mmol) in THF (30 mL) and 1 N NaOH (30 mL) was stirred overnight at room temperature. The organic solvent was removed under reduced pressure and the aqueous phase was acidified with 2 N HCl and extracted with ethyl acetate. The combined organic layers were dried over Na_2SO_4 and evaporated to dryness affording the final acids as white solids.

*9.9.1. 2-{4-[4-(2-Phenyl-1,3-oxazol-4-ylmethoxy)benzyl]phenoxy}propionic acid (**1**)*

54% Yield; mp = 185-186 °C (methanol/$CHCl_3$); IR (KBr) cm^{-1}: 3200-2800 (OH), 1731 (C=O); ESI-MS, *m/z* (%): 428 (M-1, 92), 356 ($C_{23}H_{18}NO_3^-$, 100); ^{1}H-NMR (DMSO-d_6): 1.44 (d, J=6.87, 3H, CH_3), 3.77 (s, 2H, CH_2-Ph), 4.72 (q, J=6.87, 1H, C*H*-CH_3), 4.99 (s, 2H, CH_2-O), 6.73-6.76, 6.93-6.96, 7.09-7.12, 7.50-7.53, 7.94-7.99 (m, 14H, 13 aromatics + COOH, D_2O exchanged), 8.26 (s, 1H, CH-C=C-N). ^{13}C-NMR (DMSO-d_6): δ= 173.7, 161.3, 156.7, 156.1, 138.6, 138.2, 134.5, 131.2, 130.0, 129.9, 129.6, 127.1, 126.4, 115.1, 72.0, 62.0, 18.8; HR-MS: ($[C_{26}H_{23}NO_5]$-H)$^-$, m/z 428.1493 (calc. 428.1503). Anal. Calcd for $C_{26}H_{23}NO_5$: C, 72.71%; H, 5.40%; N, 3.26%. Found: C, 73.56%; H, 5.84%; N, 3.06%.

*9.9.2. (R)-2-{4-[4-(2-Phenyl-1,3-oxazol-4-ylmethoxy)benzyl]phenoxy}propionic acid, ((R)-**1**)*

40% Yield; mp = 202-204 °C (methanol). Anal. Calcd for $C_{26}H_{23}NO_5$: C, 72.71%; H, 5.40%; N, 3.26%. Found: C, 72.56%; H, 5.34%; N, 3.44%. $[\alpha]^{20}_D$ = +34.7 (c = 1.0, DMF). HPLC (Chiralcel OD, flux 1 mL/min, λ = 254 nm, *n*-hexane/isopropanol/trifluoroacetic acid 80/20/0.2): e.e. ≥ 98%.

*9.9.3. (S)-2-{4-[4-(2-Phenyl-1,3-oxazol-4-ylmethoxy)benzyl]phenoxy}propionic acid, ((S)-**1**)* 56% Yield; mp = 203-205 °C (methanol). Anal. Calcd for $C_{26}H_{23}NO_5$: C, 72.71%; H, 5.40%; N, 3.26%. Found: C, 70.94%; H, 5.30%; N, 3.39%. $[\alpha]^{20}_D$ = -34.4 (c = 1.0, DMF). HPLC (Chiralcel OD, flux 1 mL/min, λ = 254 nm, *n*-hexane/isopropanol/trifluoroacetic acid 80/20/0.2): e.e. ≥ 99%.

*9.9.4. 2-{4-[4-(5-Methyl-2-phenyl-1,3-oxazol-4-ylmethoxy)benzyl]phenoxy}propionic acid (**2**)*

86% Yield; mp = 167-168 °C ($CHCl_3$/*n*-hexane); IR (KBr) cm^{-1}: 3200-2800 (OH), 1731 (C=O); ESI-MS, *m/z* (%):466 (M+23, 100), 444 (M+1, 19); ^{1}H-NMR (DMSO-d_6): 1.43 (d, J=6.60, 3H, C*H*$_3$-CH), 2.41 (s, 3H, CH_3-C=C-N), 3.77 (s, 2H, CH_2-Ph), 4.70 (q, J=6.60, 1H, C*H*-CH_3), 4.92 (s, 2H, CH_2-O), 6.72-6.75, 6.91-6.94, 7.06-7.12, 7.48-7.54 and 7.90-7.93 (m, 14H, 13 aromatics + COOH, D_2O exchanged). ^{13}C-NMR (DMSO-d_6): δ= 173.6, 159.2, 156.9, 156.1, 147.9, 134.6, 134.4, 132.5, 130.8 130.0, 129.9, 129.6, 127.3, 126.1, 115.2, 115.1, 71.9, 61.8, 18.7, 10.4; HR-MS: ($[C_{27}H_{25}NO_5]$-H)$^-$, m/z 442.1652 (calc. 442.1660). Anal. Calcd for $C_{27}H_{25}NO_5$: C, 73.12%; H, 5.68%; N, 3.16%. Found: C, 73.57%; H, 5.59%; N, 2.91%.

*9.9.5. 2-{4-{1-Ethyl-1-[4-(2-phenyl-1,3-oxazol-4-ylmethoxy)phenyl]propyl}phenoxy}propionic acid (**3**)*

49% Yield; mp = 140-141 °C ($CHCl_3$/*n*-hexane); IR (KBr) cm^{-1}: 3200-2800 (OH), 1730 (C=O); ESI-MS, *m/z* (%): 486 (M+1, 68), 508 (M+23, 100), 484 (M-1, 35); ^{1}H-NMR: 0.52 (t, J=6.96, 6H, 2 *CH*$_3$-CH_2), 1.44 (d, J=6.59, 3H, *CH*$_3$-CH), 1.96 (q, J=6.96, 4H, 2 *CH*$_2$-CH_3), 4.70 (q, J=6.59, 1H, *CH*-CH_3), 4.99 (s, 2H, CH_2-O), 6.70-6.73, 6.90-7.05, 7.51-7.54, 7.95-7.99 (m, 14H, 13 aromatics + COOH, D_2O exchanged), 8.27 (s, 1H, O-CH=C). ^{13}C-NMR (DMSO-d_6): δ= 173.7, 161.3, 156.1, 155.5, 141.2, 138.6, 138.3, 131.2, 129.6, 129.1, 129.0, 127.1, 126.4, 114.3, 71.9, 62.0, 48.4, 28.9, 18.8, 8.7; HR-MS: ($[C_{30}H_{31}NO_5]$-H)$^-$, m/z 484.2119 (calc. 484.2129). Anal. Calcd for $C_{30}H_{31}NO_5$: C, 74.21%; H, 6.43%; N, 2.88%. Found: C, 73.77%; H, 6.89%; N, 3.12%.

*9.9.6. 2-{4-{1-Ethyl-1-[4-(5-methyl-2-phenyl-1,3-oxazol-4-ylmethoxy)phenyl]propyl}phenoxy}-propionic acid (**4**)*

38% Yield; mp = 65-66 °C ($CHCl_3$/*n*-hexane); IR (KBr) cm^{-1}: 3200-2800 (OH), 1730 (C=O); ESI-MS, *m/z* (%): 498 (M-1, 100), 522 (M+23, 100), 425 ($C_{28}H_{28}NO_3^-$, 19); ^{1}H-NMR (DMSO-d_6): 0.53 (t, J=7.15, 6H, 2 *CH*$_3$-CH_2), 1.45 (d, J=6.87, 3H, *CH*$_3$-CH), 1.99 (q, J=7.15, 4H, 2 *CH*$_2$-CH_3), 2.42 (s, 3H, CH_3-C=C-N), 4.72 (q, J=6.87, 1H, *CH*-CH_3), 4.93 (s, 2H, CH_2-O), 6.71-7.05, 7.43-7.54 and 7.83-7.94 (m, 14H, 13 aromatics + COOH, D_2O exchanged). ^{13}C-NMR (DMSO-d_6): δ= 173.7, 159.3, 156.3, 155.5, 147.8, 141.2, 141.1, 134.7, 132.5, 131.6, 130.8, 129.7, 129.5, 129.0, 128.6, 127.9, 126.0, 114.3, 71.9, 61.7, 48.4, 28.9, 18.8, 10.4, 8.7; HR-MS: ($[C_{31}H_{33}NO_5]$-H)$^-$, m/z 498.2277 (calc. 498.2286). Anal. Calcd for $C_{31}H_{33}NO_5$ x 3 H_2O: C, 67.25%; H, 7.10%; N, 2.53%. Found: C, 68.27%; H, 6.89%; N, 2.60%.

*9.9.7. 2-{4-{1-{4-[2-(2,6-Dichloro-phenyl)-1,3-oxazol-4-ylmethoxy]phenyl}-1-ethyl-propyl}-phenoxy}-propionic acid (**5**)*

38% Yield; mp = 79-80 °C (*n*-hexane); IR (KBr) cm^{-1}: 3200-2800 (OH), 1730 (C=O); ESI-MS, *m/z* (%): 556 (M+4 -1, 16), 554 (M+2 -1, 78), 552 (M-1, 100); ^{1}H-NMR (DMSO-d_6): 0.51 (t, J=6.87 6H, 2 CH_2CH_3), 1.44 (d, J=6.60, 3H, CH-C*H*$_3$), 1.97 (q, J=6.87, 4H, 2 C*H*$_2$CH$_3$), 4.71 (q, J=6.60,

1H, C*H*-CH_3), 5.03 (s, 2H, CH_2O), 6.71-7.05 and 7.60-7.69 (m, 12H, 11 aromatics + COOH, D_2O exchanged), 8.41 (s, 1H, O-CH-C=C). ^{13}C-NMR (DMSO-d_6): δ= 173.7, 156.1, 155.5, 141.3, 141.2, 139.8, 138.9, 137.8, 135.6, 133.9, 129.1, 129.0, 128.9, 127.3, 114.9, 114.5, 114.3, 71.9, 61.9, 48.5, 29.0, 18.8, 8.7; HR-MS: ($[C_{30}H_{29}Cl_2NO_5]$-H)$^-$, m/z 552.1338 (calc. 552.1350). Anal. Calcd for $C_{30}H_{29}Cl_2NO_5$: C, 64.99%; H, 5.27%; N, 2.53%. Found: C, 66.56%; H, 5.67%; N, 2.16%.

*9.9.8. 2-{4-{1-{4-[2-(2,6-Dichloro-phenyl)-5-methyl-1,3-oxazol-4-ylmethoxy]phenyl}-1-ethyl-propyl}-phenoxy}-propionic acid (**6**)*

57% Yield; mp = 83-85 °C (*n*-hexane). IR (KBr) cm^{-1}: 3200-2800 (OH), 1730 (C=O); ESI-MS, *m/z* (%): 570 (M+4 -1, 15), 568 (M+2 -1, 72), 566 (M-1, 100); ^{1}H-NMR (DMSO-d_6): 0.52 (t, J=6.88, 6H, 2 CH_2CH_3), 1.44 (d, J=6.60, 3H, CH-CH_3), 1.98 (q, J=6.88, 4H, 2 CH_2CH_3), 2.40 (s, 3H, CH_3-C=C-N), 4.71 (q, J=6.60, 1H, C*H*-CH_3), 4.97 (s, 2H, CH_2O), 6.70-7.67 (m, 12H, 11 aromatics + COOH, D_2O exchanged). ^{13}C-NMR (DMSO-d_6): δ= 173.7, 156.2, 155.5, 153.9, 149.0, 141.3, 141.2, 135.6, 133.8, 132.1, 129.1, 129.0, 127.5, 114.7, 114.3, 71.9, 61.8, 48.5, 29.0, 18.8, 10.3, 8.7; HR-MS: ($[C_{31}H_{31}Cl_2NO_5]$-H)$^-$, m/z 566.1495 (calc. 566.1507). Anal. Calcd for $C_{31}H_{31}Cl_2NO_5$: C, 65.50%; H, 5.50%; N, 2.46%. Found: C, 66.34%; H, 5.72%; N, 2.43%.

9.10. Surface Plasmon Resonance

SPR analyses were carried out on a BIACORE 3000 instrument (GE-Healthcare) according to our previously published procedures.[39] Briefly, PPARα, PPARγ, and PPARδ surfaces were immobilized on a research−grade CM5 sensor chip (GE Healthcare) using a standard amine−coupling protocol. A densities of 3–5 kRU (1000 RU corresponds to the binding of ~ 1 ng per square mm of protein on the dextran surface) was achieved. Each compound was injected on the protein chips at five different concentrations ranging from 0.1 to 50 nM. Measurements were performed at 25 °C, using a 50 μL min^{-1} flow rate. Association and dissociation times were set at 60 s and 300 s, respectively. Interactions curves were fit to a single−site bimolecular interaction model to yield K_D. BIAevaluation software (GE Healthcare) was used for sensorgrams elaboration.

9.11. Biological Methods

Reference compounds, the medium, and other cell culture reagents were purchased from Sigma-Aldrich (Milan, Italy) and Invitrogen (Basel, Switzerland).

9.12. Plasmids

The expression vectors expressing the chimeric receptors containing the yeast GAL4-DNA binding domain fused to either the human PPARα, PPARγ, PPARδ or FXR ligand binding domain (LBD) and the reporter plasmid for these GAL4 chimeric receptors (pGAL5TKpGL3) containing five repeats of the GAL4 response elements upstream of a minimal thymidine kinase promoter upstream to the luciferase gene were described previously.[64]

9.13. Cell Culture and Transfections

Human hepatoblastoma cell line HepG2 (Interlab Cell Line Collection, Genoa, Italy) was cultured in Minimum Essential Medium (MEM) containing 10% heat-inactivated foetal bovine serum, 100 U of penicillin G·mL^{-1} and 100 μg of streptomycin sulfate·mL^{-1} at 37°C in a humidified atmosphere of 5% CO_2. For transactivation assays, 10^5 cells/well were seeded in a 24-well plate and transfections were performed after 24 hs with the CAPHOS®, a calcium-phosphate method, according to the manufacturer's guidelines. Cells were transfected with expression plasmids encoding the fusion protein GAL4-PPARα-LBD, GAL4-PPARγ-LBD, GAL4-PPARδ-LBD or GAL4-FXR-LBD (30 ng), pGAL5TKpGL3 (100 ng), pCMVβgal (250 ng). Four hours after transfection, cells were treated for 20 hs with the indicated ligands in triplicate. Luciferase activity in cell extracts was then determined by a luminometer (VICTOR^3 V Multilabel Plate Reader PerkinElmer). β-Galactosidase activity was determined using ortho-nitro-phenyl-β-D-galactopyranoside as described previously.[65] All transfection experiments were repeated at least twice.

9.14. Real-time PCR

HepG2 cells in serum-free medium were incubated for 24 hs with 1 μM (*R*)-**1**, (*S*)-**1**, (*R,S*)-**2** or 50 μM Wy-14,643. Total RNA was extracted from $1x10^6$ cells; reverse transcription and real-time PCR were performed as previously reported.[66] Specific TaqMan Gene Expression Assays for human CPT1, CAC, PPARα and β-actin (Hs00912671m1, Hs01088810g1, Hs00947536_m1 and Hs00357333g1, respectively) were purchased from Life technologies. All transcript levels were normalized against the β-actin expression levels.

*9.15. Cell culture, treatment with compounds (R)-**1**, (S)-**1** or (R,S)-**2** and viability evaluation by counting*

The human colon adenocarcinoma derived cells HT-29 and human kidney HEK293T cells were grown as a monolayer in D-MEM containing 10% FBS, 1% penicillin-streptomycin and 1% L-glutamine and cultured in 100 mm plates at 37°C in a 5% CO_2 humidified atmosphere up to 70-80% confluence. (*R*)-**1**, (*S*)-**1** or (*R,S*)-**2** or rosiglitazone were dissolved in DMSO as vehicle and treatments were carried out in the presence of 10% FBS containing 1% penicillin-streptomycin and 1% L-glutamine. In all experiments, the DMSO final concentration in the medium was less than 0.1%. To evaluate cell growth after exposure to test compounds, cells were plated in 12-well plates at 10^6 cells/cm^2 density (24-well plates at 10^5 cells/cm^2 density). After treatment, cells were washed with PBS, trypsinized and collected in culture medium. Cell counting was performed by means of a Bürker's hemocytometer. Three counts for each well were made and the mean value and the standard deviation calculated.

9.16. Top-FLASH reporter assay

The Top-FLASH reporter plasmid was transiently transfected into HEK293 cells with Lipofectamine 2000 (Invitrogen, Carlsbad, CA, USA) in 24-well plates. To activate the Wnt/β-catenin pathway, cells were treated with 20 mM LiCl alone or in combination with 1 μM rosiglitazone or compounds (*R*)-**1**, (*S*)-**1** or (*R,S*)-**2** for 24 hs. Luciferase activity was determined in the cell extracts 48 hs after transfection. All experiments were performed three times with triplicate replicates.

9.17. Protein extract preparation and western blotting analysis

HepG2 cells were incubated for 48 hs with 1 μM (*R*)-**1**, (*S*)-**1**, (*R,S*)-**2** or 50 μM Wy-14,643, starting 24 hs after having been depleted of serum. Proteins were electroblotted onto nitrocellulose membranes (Bio-Rad) and subsequently treated with anti-CPT1 (ARP44796_P050, Aviva Systems Biology), anti-CAC, [28] anti-PPARα (sc-9000, Santa Cruz) and anti-β-actin (sc-58619, Santa Cruz) antibodies. The immunoreaction was detected by the Immobilon™ Western Chemiluminescent HRP Substrate (Millipore).

Treated and untreated HT-29 cells were lysed in Ripa buffer (150 mM NaCl, 50 mM Tris–HCl, pH 7.6, 10 mM EDTA, 1% NP-40) containing also a protease inhibitors cocktail (AEBSF, Aprotinin, Bestatin hydrochloride, E-64, Leupeptin hemisulfate salt, Pepstatin A) and then centrifugated at 13,000 rpm for 10 min, at 4 °C. Supernatant containing total proteins was quantified and 80 μg of each sample were used for western blot experiments. Antibodies against $p21^{waf1/cip1}$, cyclin D1, c-myc and β-actin were purchased from Santa Cruz Biotechnology. The relative intensity of protein bands was measured using the Molecular Imager Chemi-Doc imaging system (Bio-Rad, Hercules CA, USA) and evaluated by the Quantity One software (Bio-Rad, Hercules CA, USA).

9.18. Assessment of mitochondrial mass

Changes in mitochondrial mass were evaluated by performing fluorescence microscopy (Floid Cell Imaging Station, Life Technologies). We used CellLight® Mitochondria-GFP BacMam 2.0 (Life Technologies) - a fusion construct of the Leader sequence of E1 alpha pyruvate dehydrogenase and green fluorescent protein (GFP) providing accurate and specific targeting to live cell mitochondria independently of mitochondrial membrane potential - following the manufacturer's instructions. Briefly, 60% confluent HepG2 cells in serum-free medium were transduced with CellLight®Mitochondria-GFP BacMam 2.0 (50 particles per cell) and treated with 1 μM (*R*)-**1**, (*S*)-**1**, (*R,S*)-**2** or 50 μM Wy-14,643 for 24 h. Then, cells were used for microscopy analysis by GFP filter set (excitation at 485 nm and emission at 535 nm). Images were captured with X20 lens and were processed identically. In another set of experiments, HepG2 cells in serum-free medium were transduced with CellLight® Mitochondria-GFP BacMam 2.0 in the presence or absence of 1 μM (*R*)-**1**, (*S*)-**1**, (*R,S*)-**2** or 50 μM Wy-14,643 for 24 hs, rinsed twice with PBS and lysed in buffer containing 10% SDS and 0.1 M Tris (pH 7.5). Cell extract fluorescence was then measured using GloMax plate reader (Promega) with excitation at 475 nm and emission at 500-550 nm.

9.19. Computational chemistry

Molecular modeling and graphics manipulations were performed using Maestro 10.1 (Schrödinger)[67] and UCSF-Chimera 1.8.1 software packages [68] running on a E4 Computer Engineering E1080 workstation provided of a Intel Core i7-930 Quad-Core processor. GOLD 5.2.2 [41] was used for all docking calculations. Figures were generated using Pymol 1.0.[69]

9.20. Protein and Ligand Preparation

The crystal structures of PPARα and PPARγ complexed with the partial agonists aleglitazar (PDB ID: 3G8I) [45] and LT127 (PDB ID: 2I4P),[44] respectively, were download from the PDB Bank,[70] and employed for the automated docking studies. The proteins were processed through

the Protein Preparation Wizard in Maestro.[71] The right bond orders as well as charges and atom types were assigned and the hydrogen atoms were added to both proteins. Arginine and lysine side chains were considered as cationic at the guanidine and ammonium groups, and the aspartic and glutamic residues were considered as anionicat the carboxylate groups.

For PPARγ, all crystallographic water molecules were deleted. For PPARα, the two well-defined water molecules bridging between the T279 OH group on helix 3 and the main chain C=O oxygen of L331 on β-sheet, were included in the docking experiments. Imidazole rings of H440 into PPARα and H449 and H323 into PPARγ were set in their N^{ε} 2-H (N *tau*-H) tautomeric state. Moreover, an exhaustive sampling of the orientations of groups, whose H-bonding network needs to be optimized, was performed. Finally, the protein structures were refined with a restrained minimization with the OPLS2005 force field [72] by imposing a 0.3 Å root-mean-square deviation (rmsd) limit as the constraint.

The structures of (*R*)-**1** and (*S*)-**1** enantiomers were built using the fragment dictionary of Maestro and preprocessed with LigPrep 3.3 [73] which prepares the ligands in multiple protonation and tautomerization states at a neutral pH. Ligands were then optimized by Macromodel 10.7 [74] using the MMFFs force field with the steepest descent (1000 steps) followed by truncated Newton conjugate gradient (500 steps) methods. Partial atomic charges were computed using the OPLS-AA force field.

9.21. Docking Simulations

Docking of (*R*)-**1** and (*S*)-**1** to both PPARγ and PPARα was performed with the GOLD software, which uses a genetic algorithm (GA) for determining the docking modes of ligands and proteins. The coordinates of the co-crystallized ligands aleglitazar and LT127 were chosen as active-site origin. The active-site radius was set equal to 8 Å. Each GA run used the default parameters of 100 000 genetic operations on an initial population of 100 members divided into five

subpopulations, with weights for crossover, mutation, and migration being set to 95, 95, and 10, respectively. For PPARα, the two crystal waters connecting T279 and L331 via H-bonds were allowed to toggle on during the individual docking runs (i.e., these waters were present in the binding site).[75] GOLD allows a user-definable number of GA runs per ligand, each of which starts from a different orientation. For these experiments, the number of GA runs was set to 200 without the option of early termination, and scoring of the docked poses was performed with the original ChemPLP scoring function rescoring with ChemScore.[38,43,76] The final receptor–ligand complex for each ligand was chosen interactively by selecting the highest scoring pose that was consistent with experimentally-derived information about the binding mode of the ligand.

Funding: This work was supported by the Università degli Studi di Bari "Aldo Moro" (F.L.) and the Ministero dell'Istruzione, Università e Ricerca (MIUR-PRIN 2010-2011 prot. 2010W7YRLZ_003) (A.L.).

Supporting information

Proton (^{1}H) and carbon (^{13}C) NMR spectra of final compounds.

References

[1] J.P. Berger, T.E. Akiyama, P.T. Meinke, PPARs: therapeutic targets for metabolic disease, Trends Pharmacol. Sci. 26 (2005) 244−251.

[2] B. Desvergne, W. Wahli, Peroxisome proliferator-activated receptors: nuclear control of metabolism, Endocr. Rev. 20 (1999) 649−688.

[3] S.A. Kliewer, S.S. Sundseth, S.A. Jones, P.J. Brown, G.B. Wisely, C.S. Koble, P. Devchand, W. Wahli, T.M. Willson, J.M. Lenhard, J.M. Lehmann, Fatty acids and eicosanoids regulate gene expression through direct interactions with peroxisome proliferator-activated receptors alpha and gamma, Proc. Natl. Acad. Sci. U. S. A. 94 (1997) 4318−4323.

4] L. Nagy, J.W. Schwabe, Mechanism of the nuclear receptor molecular switch. Trends Biochem. Sci. 29 (2004) 317−324.

[5] K.W. Nettles, G.L. Greene, Ligand control of coregulator recruitment to nuclear receptors, Annu. Rev. Physiol. 67 (2005) 309−333.

[6] J.P. Renaud, D. Moras, Structural studies on nuclear receptors, Cell. Mol. Life Sci. 57 (2000) 1748−1769.

[7] M. Elisaf, Effects of fibrates on serum metabolic parameters, Curr. Med. Res. Opin. 18 (2002) 269−276.

[8] B. Staels, J. Dallongeville, J. Auwerx, K. Schoonjans, E. Leitersdorf, J.-C.Fruchart, Mechanism of action of fibrates on lipid and lipoprotein metabolism, Circulation 98 (1998) 2088−2093.

[9] I.W. Campbell, The Clinical Significance of PPARgamma Agonism, Curr. Mol. Med. 5 (2005) 349−363.

[10] A. Grey, Skeletal consequences of thiazolidinedione therapy, Osteoporos. Int. 19 (2008) 129−137.

[11] B.C. Hansen, X.T. Tigno, A. Benardeau, M. Meyer, E. Sebokova, J. Mizrahi, Effects of aleglitazar, a balanced dual peroxisome proliferator-activated receptor alpha/gamma agonist on glycemic and lipid parameters in a primate model of the metabolic syndrome, Cardiovasc. Diabetol. 10 (2011) 7.

[12] A. Rubenstrunk, R. Hanf, D.W. Hum, J.-C. Fruchart, B. Staels, Safety issues and prospects for future generations of PPAR modulators, Biochim. Biophys. Acta 1771 (2007) 1065−1081.

[13] B.G. Shearer, A.N. Billin, The next generation of PPAR drugs: do we have the tools to find them? Biochim. Biophys. Acta 1771 (2007) 1082−1093.

[14] K.B. Pouwels, K. van Grootheest, The rosiglitazone decision process at FDA and EMA. What should we learn? Int. J. Risk. Saf. Med. 24 (2012) 73−80.

[15] T. Kaserer, V. Obermoser, A. Weninger, R. Gust, D. Schuster, Evaluation of selected 3D virtual screening tools for the prospective identification of peroxisome proliferator-activated receptor PPARgamma partial agonists, Eur. J. Med. Chem. 124, (2016) 49−62.

[16] V. Obermoser, M.E. Urban, M.S. Murgueitio, G. Wolber, U. Kintscher, R. Gust, New telmisartan-derived PPARgamma agonists: Impact of the 3D-binding mode on the pharmacological profile, Eur. J. Med. Chem. 124, (2016) 138−152.

[17] V. Obermoser, R. Mauersberger, D. Schuster, M. Czifersky, M. Lipova, M. Siegl, U. Kintscher, R. Gust, Importance of 5/6-aryl substitution on the pharmacological profile of 4'-((2-propyl-1H-benzo[d]imidazol-1-yl)methyl)-[1,1'-biphenyl]-2-carboxylic acid derived PPARgamma agonists, Eur. J. Med. Chem. In Press, Available online 25 November 2016.

[18] T. Coll, R. Rodriguez-Calvo, E. Barroso, L. Serrano, E. Eyre, X. Palomer, M. Vazquez-Carrera, Peroxisome proliferator-activated receptor (PPAR) beta/delta: a new potential therapeutic target for the treatment of metabolic syndrome, Curr. Mol. Pharmacol. 2 (2009) 46−55.

[19] C. Fievet, J.-C. Fruchart, B. Staels, PPARalpha and PPARgamma dual agonists for the treatment of type 2 diabetes and the metabolic syndrome, Curr. Opin. Pharmacol. 6 (2006) 606−614.

[20] M. Heald, M.A. Cawthorne, Dual acting and pan-PPAR activators as potential anti-diabetic therapies, Handb. Exp. Pharmacol. 203 (2011) 35−51.

[21] R. Agrawal, The first approved agent in the Glitazar's Class: Saroglitazar, Curr. Drug Targets 15 (2014) 151−155.

[22] M.F. Boehm, P. Fitzgerald, A. Zou, M.G. Elgort, E.D. Bischoff, L. Mere, D.E. Mais, R.P. Bissonnette, R.A. Heyman, A.M. Nadzan, M. Reichman, E.A. Allegretto, Novel nonsecosteroidal vitamin D mimics exert VDR-modulating activities with less calcium mobilization than 1,25-dihydroxyvitamin D3, Chem. Biol. 6 (1999) 265−275.

[23] S. Hosoda, A. Tanatani, K. Wakabayashi, Y. Nakano, H. Miyachi, K. Nagasawa, Y. Hashimoto, Ligands with dual vitamin D3-agonistic and androgen-antagonistic activities, Bioorg. Med. Chem. Lett. 15 (2005) 4327−4331.

[24] M. Kainuma, J. Kasuga, S. Hosoda, K. Wakabayashi, A. Tanatani, K. Nagasawa, H. Miyachi, M. Makishima, Y. Hashimoto, Diphenylmethane skeleton as a multi-template for nuclear receptor ligands: preparation of FXR and PPAR ligands, Bioorg. Med. Chem. Lett. 16 (2006) 3213−3218.

[25] B. De Filippis, P. Linciano, A. Ammazzalorso, C. Di Giovanni, M. Fantacuzzi, L. Giampietro, A. Laghezza, C. Maccallini, P. Tortorella, A. Lavecchia, F. Loiodice, R. Amoroso, Structural development studies of PPARs ligands based on tyrosine scaffold, Eur. J. Med. Chem. 89 (2015) 817−825.

[26] M. Düfer, K. Hörth, R. Wagner, B. Schittenhelm, S. Prowald, T. Wagner, J. Oberwinkler, R. Lukowski, F. Gonzalez, P. Krippeit-Drews, G. Drews, Bile acids acutely stimulate insulin secretion

of mouse cells via Farnesoid X Receptor activation and KATP channel inhibition, Diabetes 6 (2012) 1479−1489.

[27] M. Düfer, K. Hörth, P. Krippeit-Drews, G. Drews, The significance of the nuclear farnesoid X receptor (FXR) in β cell function, Islets 5 (2012) 333−338.

[28] B. Renga, A. Mencarelli, P. Vavassori, V. Brancaleone, S. Fiorucci, The bile acid sensor FXR regulates insulin transcription and secretion, Biochim. Biophys. Acta 3 (2010) 363−372.

[29] P. Sarraf, E. Muller, D. Jones, S. Holden, S. Tomoyasu, H.P. Koeffler, Differentiation and reversal of malignant changes in colon cancer through PPARγ differentiation, Nat. Med. 4 (1998) 1046−1052.

[30] J.I. Hisatake, T. Ikezoe, M. Carey, S. Holden, S. Tomoyasu, H.P. Koeffler, Downregulation of prostate-specific antigen expression by ligands for peroxisome proliferator-activated receptor γ in human prostate cancer, Cancer Res. 60 (2000) 5494−5498.

[31] H. Liu, C. Zang, M.H. Fenner, K. Possinger, E. Elstner, PPAR gamma ligands and ATRA inhibit the invasion of human breast cancer cells in vitro, Breast Cancer Res. Treat. 79 (2003) 63−74.

[32] C. Grommes, G.E. Landreth, M.T. Heneka, Antineoplastic effects of peroxisome proliferator-activated receptor gamma agonists, Lancet Oncol. 5 (2004) 419−429.

[33] S. Theocharis, A. Margeli, P. Vielh, G. Kouraklis, Peroxisome proliferator-activated receptor-gamma ligands as cell-cycle modulators, Cancer Treat. Rev. 30 (2004) 545−554.

[34] A. Gutgesell, G. Wen, B. Konig, A. Koch, J. Spielmann, G.I. Stangl, K. Eder, R. Ringseis, Mouse carnitine-acylcarnitine translocase (CACT) is transcriptionally regulated by PPARalpha and PPARdelta in liver cells, Biochim. Biophys. Acta 1790 (2009) 1206−1216.

[35] V. Iacobazzi, P. Convertini, V. Infantino, P. Scarcia, S. Todisco, F. Palmieri, Statins, fibrates and retinoic acid upregulate mitochondrial acylcarnitine carrier gene expression, Biochem. Biophys. Res. Commun. 388 (2009) 643−647.

[36] C. Indiveri, V. Iacobazzi, A. Tonazzi, N. Giangregorio, V. Infantino, P. Convertini, L. Console, F. Palmieri, The mitochondrial carnitine/acylcarnitine carrier: function, structure and physiopathology, Mol. Aspects Med. 32 (2011) 223−233.

[37] A. Laghezza, G. Pochetti, A. Lavecchia, G. Fracchiolla, S. Faliti, L. Piemontese, C. Di Giovanni, V. Iacobazzi, V. Infantino, R. Montanari, D. Capelli, P. Tortorella, F. Loiodice, New 2-(aryloxy)-3-phenylpropanoic acids as peroxisome proliferator-activated receptor alpha/gamma dual agonists able to upregulate mitochondrial carnitine shuttle system gene expression, J. Med. Chem. 56 (2013) 60−72.

[38] (a) A. Carrieri, M. Giudici, M. Parente, M. De Rosas, L. Piemontese, G. Fracchiolla, A. Laghezza, P. Tortorella, G. Carbonara, A. Lavecchia, F. Gilardi, M. Crestani, F. Loiodice, Molecular determinants for nuclear receptors selectivity: chemometric analysis, dockings and site-directed mutagenesis of dual peroxisome proliferator-activated receptors alpha/gamma agonists, Eur. J. Med. Chem. 63 (2013) 321−332. (b) G. Fracchiolla, A. Laghezza, L. Piemontese, M. Parente, A. Lavecchia, G. Pochetti, R. Montanari, C. Di Giovanni, G. Carbonara, P. Tortorella, E. Novellino, F. Loiodice, Synthesis, biological evaluation and molecular investigation of fluorinated peroxisome proliferator-activated receptors alpha/gamma dual agonists, Bioorg. Med. Chem. 20 (2012) 2141−2151. (c) A. Pinelli, C. Godio, A. Laghezza, N. Mitro, G. Fracchiolla, V. Tortorella, A. Lavecchia, E. Novellino, J.-C. Fruchart, B. Staels, M. Crestani, F. Loiodice, Synthesis, biological evaluation, and molecular modeling investigation of new chiral fibrates with PPARalpha and PPARgamma agonist activity, J. Med. Chem. 48 (2005) 5509−5519. (d) L. Porcelli, F. Gilardi, A. Laghezza, L. Piemontese, N. Mitro, A. Azzariti, F. Altieri, L. Cervoni, G. Fracchiolla, M. Giudici, U. Guerrini, A. Lavecchia, R. Montanari, C. Di Giovanni, A. Paradiso, G. Pochetti, G.M. Simone, P. Tortorella, M. Crestani, F. Loiodice, Synthesis, characterization and biological evaluation of ureidofibrate-like derivatives endowed with peroxisome proliferator-activated receptor activity, J. Med. Chem. 55 (2012) 37−54.

[39] F. Dal Piaz, A. Vassallo, A. Temraz, R. Cotugno, M.A. Belisario, G. Bifulco, M.G. Chini, C. Pisano, N. De Tommasi, A. Braca, A chemical–biological study reveals C9-type iridoids as novel heat shock protein 90 (HSP90) inhibitors, J. Med. Chem. 56 (2013) 1583−1595.

[40] F. Dal Piaz, A. Tosco, D. Eletto, A.L. Piccinelli, O. Moltedo, S. Franceschelli, G. Sbardella, P. Remondelli, L. Rastrelli, L. Vesci, C. Pisano, N. De Tommasi, The identification of a novel natural activator of p300 histone acetyltransferase provides new insights into the modulation mechanism of this enzyme, ChemBioChem. 11 (2010) 818−827.

[41] (a) GOLD, version 5.2.2. CCDC Software Limited: Cambridge, U.K. (2008). (b) G. Jones, P. Willett, R.C. Glen, A.R. Leach, R. Taylor, Development and validation of a genetic algorithm for flexible docking, J. Mol. Biol. 267 (1997) 727–748.

[42] M.L. Verdonk, I. Giangreco, R.J. Hall, O. Korb, P.N. Mortenson, C.W. Murray, Docking performance of fragments and druglike compounds, J. Med. Chem. 54 (2011) 5422−5431.

[43] M.L. Verdonk, J.C. Cole, M.J. Hartshorn, C.W. Murray, R.D. Taylor, Improved protein-ligand docking using GOLD, Proteins 52 (2003) 609−623.

[44] G. Pochetti, C. Godio, N. Mitro, D. Caruso, A. Galmozzi, S. Scurati, F. Loiodice, G. Fracchiolla, P. Tortorella, A. Laghezza, A. Lavecchia, E. Novellino, F. Mazza, M. Crestani, Insights into the mechanism of partial agonism: crystal structures of the peroxisome proliferator-activated receptor gamma ligand-binding domain in the complex with two enantiomeric ligands, J. Biol. Chem. 282 (2007) 17314−17324.

[45] A. Benardeau, J. Benz, A. Binggeli, D. Blum, M. Boehringer, U. Grether, H. Hilpert, B. Kuhn, H.P. Marki, M. Meyer, K. Puntener, S. Raab, A. Ruf, D. Schlatter, P. Mohr, Aleglitazar, a new, potent, and balanced dual PPARalpha/gamma agonist for the treatment of type II diabetes, Bioorg. Med. Chem. Lett. 19 (2009) 2468−2473.

[46] (a) J.B. Bruning, M.J. Chalmers, S. Prasad, S.A. Busby, T.M. Kamenecka, Y. He, K.W. Nettles, P.R. Griffin, Partial agonists activate PPARgamma using a helix 12 independent

mechanism, Structure 15 (2007) 1258−1271. (b) M.J. Chalmers, S.A. Busby, B.D. Pascal, M.R. Southern, P.R. Griffin, A two-stage differential hydrogen deuterium exchange method for the rapid characterization of protein/ligand interactions, J. Biomol. Tech. 18 (2007) 194−204. (c) Y. Hamuro, S.J. Coales, J.A. Morrow, K.S. Molnar, S.J. Tuske, M.R. Southern, P.R. Griffin, Hydrogen/deuterium-exchange (H/D-Ex) of PPARgamma LBD in the presence of various modulators, Protein Sci. 15 (2006) 1883−1892. (d) R.T. Nolte, G.B. Wisely, S. Westin, J.E. Cobb, M.H. Lambert, R. Kurokawa, M.G. Rosenfeld, T.M. Willson, C.K. Glass, M.V. Milburn, Ligand binding and co-activator assembly of the peroxisome proliferator-activated receptor-gamma, Nature 395 (1998) 137−143.

[47] L. Gelman, J.N. Feige, B. Desvergne, Molecular basis of selective PPARgamma modulation for the treatment of Type 2 diabetes, Biochim. Biophys. Acta 1771 (2007) 1094−1107.

[48] (a) P. Cronet, J.F. Petersen, R. Folmer, N. Blomberg, K. Sjoblom, U. Karlsson, E.L. Lindstedt, K. Bamberg, Structure of the PPARalpha and -gamma ligand binding domain in complex with AZ 242; ligand selectivity and agonist activation in the PPAR family, Structure 9 (2001) 699−706. (b) J. Li, L.J. Kennedy, Y. Shi, S. Tao, X.Y. Ye, S.Y. Chen, Y. Wang, A.S. Hernandez, W. Wang, P.V. Devasthale, S. Chen, Z. Lai, H. Zhang, S. Wu, R.A. Smirk, S.A. Bolton, D.E. Ryono, H. Zhang, N.K. Lim, B.C. Chen, K.T. Locke, K.M. O'Malley, L. Zhang, R.A. Srivastava, B. Miao, D.S. Meyers, H. Monshizadegan, D. Search, D. Grimm, R. Zhang, T. Harrity, L.K. Kunselman, M. Cap, P. Kadiyala, V. Hosagrahara, L. Zhang, C. Xu, Y.X. Li, J.K. Muckelbauer, C. Chang, Y. An, S.R. Krystek, M.A. Blanar, R. Zahler, R. Mukherjee, P.T. Cheng, J.A.Tino, Discovery of an oxybenzylglycine based peroxisome proliferator activated receptor alpha selective agonist 2-((3-((2-(4-chlorophenyl)-5-methyloxazol-4-yl)methoxy)benzyl)(methoxycarbonyl)am ino)acetic acid (BMS-687453), J. Med. Chem. 53 (2010) 2854−2864. (c) M.L. Sierra, V. Beneton, A.B. Boullay, T. Boyer, A.G. Brewster, F. Donche, M.C. Forest, M.H. Fouchet, F.J. Gellibert, D.A. Grillot, M.H. Lambert, A. Laroze, C. Le Grumelec, J.M. Linget, V.G. Montana, V.L. Nguyen, E. Nicodeme, V. Patel, A. Penfornis, O. Pineau, D. Pohin, F. Potvain, G. Poulain, C.B. Ruault, M.

Saunders, J. Toum, H.E. Xu, R.X. Xu, P.M. Pianetti, Substituted 2-[(4-aminomethyl)phenoxy]-2-methylpropionic acid PPARalpha agonists. 1. Discovery of a novel series of potent HDLc raising agents, J. Med. Chem. 50 (2007) 685−695. (d) W. Wang, P. Devasthale, D. Farrelly, L. Gu, T. Harrity, M. Cap, C. Chu, L. Kunselman, N. Morgan, R. Ponticiello, R. Zebo, L. Zhang, K. Locke, J. Lippy, K. O'Malley, V. Hosagrahara, L. Zhang, P. Kadiyala, C. Chang, J. Muckelbauer, A.M. Doweyko, R. Zahler, D. Ryono, N. Hariharan, P.T. Cheng, Discovery of azetidinone acids as conformationally-constrained dual PPARalpha/gamma agonists, Bioorg. Med. Chem. Lett. 18 (2008) 1939−1944. (e) H.E. Xu, M.H. Lambert, V.G. Montana, K.D. Plunket, L.B. Moore, J.L. Collins, J.A. Oplinger, S.A. Kliewer, R.T. Jr. Gampe, D.D. McKee, J.T. Moore, T.M. Willson, Structural determinants of ligand binding selectivity between the peroxisome proliferator-activated receptors, Proc. Natl. Acad. Sci. U. S. A. 98 (2001) 13919−13924.

[49] E.A. Meyer, R.K. Castellano, F. Diederich, Interactions with aromatic rings in chemical and biological recognition, Angew. Chem. Int. Ed. Engl. 42 (2003) 1210−1250.

[50] Y. Bren-Mattison, V. Van Putten, D. Chan, R. Winn, M.W. Geraci, R.A. Nemenoff, Peroxisome proliferator-activated receptor-gamma (PPARgamma) inhibits tumorigenesis by reversing the undifferentiated phenotype of metastatic non-small-cell lung cancer cells (NSCLC), Oncogene 24 (2005) 1412−1422.

[51] (a) E.R. Fearon, B. Vogelstein, A genetic model for colorectal tumorigenesis, Cell 61 (1990) 759−67. (b) S.M. Powell, N. Zilz, Y. Beazer-Barclay, T.M. Bryan, S.R. Hamilton, S.N. Thibodeau, B. Vogelstein, K.W. Kinzler, APC mutations occur early during colorectal tumorigenesis, Nature 359 (1992) 235−237. (c) L. Sabatino, M. Pancione, C. Votino, T. Colangelo, A. Lupo, E. Novellino, A. Lavecchia, V. Colantuoni, Emerging role of the beta-catenin-PPARgamma axis in the pathogenesis of colorectal cancer, World J. Gastroenterol. 20 (2014) 7137−7151.

[52] R.S. Jope, Lithium and GSK-3: one inhibitor, two inhibitory actions, multiple outcomes, Trends Pharmacol. Sci. 24 (2003) 441−443.

[53] W. Wang, L. Heideman, C.S. Ching, J.C. Pelling, K.J. Koehler, D.F. Birt, Cell-cycle arrest at G2/M and growth inhibition by apigenin in human colon carcinoma cell lines, Mol. Carcinog. 28 (2000) 102−110.

[54] K. Lee, J. Kerner, C.L. Hoppel, Mitochondrial carnitine palmitoyltransferase 1a (CPT1a) is part of an outer membrane fatty acid transfer complex, J. Biol. Chem. 286 (2011) 25655−25662.

[55] A.C. Rufer, R. Thoma, M. Hennig, Structural insight into function and regulation of carnitine palmitoyltransferase, Cell. Mol. Life Sci. 66 (2009) 2489−2501.

[56] K. Zeth, M. Thein, Porins in prokaryotes and eukaryotes: common themes and variations, Biochem. J. 431 (2010) 13−22.

[57] R.R. Ramsay, R.D. Gandour, F.R. van der Leij, Molecular enzymology of carnitine transfer and transport, Biochim. Biophys. Acta 1546 (2001) 21−43.

[58] (a) S. Kersten, Integrated physiology and systems biology of PPARalpha, Mol. Metab. 3 (2014) 354−371. (b) S. Kersten, J. Seydoux, J.M. Peters, F.J. Gonzalez, B. Desvergne, W. Wahli, Peroxisome proliferator-activated receptor alpha mediates the adaptive response to fasting, J. Clin. Invest. 103 (1999) 1489−1498.

[59] M. Seo, I. Inoue, M. Ikeda, T. Nakano, S. Takahashi, S. Katayama, T. Komoda, Statins Activate Human PPARalpha Promoter and Increase PPARalpha mRNA Expression and Activation in HepG2 Cells, PPAR Res. 2008 (2008) 316306.

[60] N.R. Madamanchi, M.S. Runge, Mitochondrial dysfunction in atherosclerosis, Circ. Res. 100 (2007) 460−473.

[61] J.A. Kim, Y. Wei, J.R. Sowers, Role of mitochondrial dysfunction in insulin resistance, Circ. Res. 102 (2008) 401−414.

[62] M. Zamora, J.A. Villena, Targeting mitochondrial biogenesis to treat insulin resistance, Curr. Pharm. Des. 20 (2014) 5527−5557.

[63] J.G. Duncan, J.L. Fong, D.M. Medeiros, B.N. Finck, D.P. Kelly, Insulin-resistant heart exhibits a mitochondrial biogenic response driven by the peroxisome proliferator-activated receptor-alpha/PGC-1alpha gene regulatory pathway, Circulation 115 (2007) 909−917.

[64] E. Raspe, L. Madsen, A.M. Lefebvre, I. Leitersdorf, L. Gelman, J. Peinado-Onsurbe, J. Dallongeville, J.-C. Fruchart, R. Berge, B. Staels, Modulation of rat liver apolipoprotein gene expression and serum lipid levels by tetradecylthioacetic acid (TTA) via PPARalpha activation, J. Lipid Res. 40 (1999) 2099−2110.

[65] T. Hollon, F.K. Yoshimura, Variation in enzymatic transient gene expression assays, Anal. Biochem. 182 (1989) 411−418.

[66] (a) P. Convertini, F. Tramutola, V. Iacobazzi, P. Lupattelli, L. Chiummiento, V. Infantino, Permethylated Anigopreissin A inhibits human hepatoma cell proliferation by mitochondria-induced apoptosis, Chem. Biol. Interact. 237 (2015) 1−8. (b) V. Infantino, V. Iacobazzi, A. Menga, M.L. Avantaggiati, F. Palmieri, A key role of the mitochondrial citrate carrier (SLC25A1) in TNFalpha- and IFNgamma-triggered inflammation, Biochim. Biophys. Acta 1839 (2014) 1217−1225.

[67] MAESTRO, version 10.1. Schrödinger, LLC, New York, NY (2015).

[68] C.C. Huang, G.S. Couch, E.F. Pettersen, T.E. Ferrin, Chimera: an extensible molecular modelling application constructed using standard components, http://www.cgl.ucsf.edu/chimera. Pac. Symp. Biocomput. 1996, 724.

[69] W.L. DeLano, "The PyMOL Molecular Graphics System." http://www.pymol.org/. ΔεΛανο Scientific LLC, San Carlos, CA, USA.

[70] H.M. Berman, T. Battistuz, T.N. Bhat, W.F. Bluhm, P.E. Bourne, K. Burkhardt, Z. Feng, G.L. Gilliland, L. Iype, S. Jain, P. Fagan, J. Marvin, D. Padilla, V. Ravichandran, B. Schneider, N. Thanki, H. Weissig, J.D. Westbrook, C. Zardecki, The Protein Data Bank. Acta Crystallogr. D Biol. Crystallogr. 58 (2002) 899−907.

[71] G.M. Sastry, M. Adzhigirey, T. Day, R. Annabhimoju, W. Sherman, Protein and ligand preparation: parameters, protocols, and influence on virtual screening enrichments, J. Comput. Aided Mol. Des. 27 (2013) 221−234.

[72] Z. Song, F.A. Kovacs, J. Wang, J.K. Denny, S.C. Shekar, J.R. Quine, T.A. Cross, Transmembrane domain of M2 protein from influenza A virus studied by solid-state (15)N polarization inversion spin exchange at magic angle NMR, Biophys. J. 79 (2000) 767−775.

[73] LIGPREP, version 3.3. Schrödinger, LLC, New York, NY (2015).

[74] MACROMODEL, version 10.7. Schrödinger, LLC, New York, NY (2015).

[75] M.L. Verdonk, G. Chessari, J.C. Cole, M.J. Hartshorn, C.W. Murray, J.W. Nissink, R.D. Taylor, R. Taylor, Modeling water molecules in protein-ligand docking using GOLD, J. Med. Chem. 48 (2005) 6504−6515.

[76] (a) N. Micale, R. Ettari, A. Lavecchia, C. Di Giovanni, K. Scarbaci, V. Troiano, S. Grasso, E. Novellino, T. Schirmeister, M. Zappalà, Development of peptidomimetic boronates as proteasome inhibitors, Eur. J. Med. Chem. 64 (2013) 23−34. (b) G. Fracchiolla, A. Laghezza, L. Piemontese, P. Tortorella, F. Mazza, R. Montanari, G. Pochetti, A. Lavecchia, E. Novellino, S. Pierno, D. Conte Camerino, F. Loiodice, New 2-aryloxy-3-phenyl-propanoic acids as peroxisome proliferator-activated receptors alpha/gamma dual agonists with improved potency and reduced adverse effects on skeletal muscle function, J. Med. Chem. 52 (2009) 6382−6393. (c) M.G. Perrone, P. Vitale, P. Malerba, A. Altomare, R. Rizzi, A. Lavecchia, C. Di Giovanni, E. Novellino, A. Scilimati, Diarylheterocycle core ring features effect in selective COX-1 inhibition, ChemMedChem 7 (2012) 629−641. (d) K. Scarbaci, V. Troiano, N. Micale, R. Ettari, L. Tamborini, C. Di Giovanni, C. Cerchia, S. Grasso, E. Novellino, T. Schirmeister, A. Lavecchia, M. Zappalà, Identification of a new series of amides as non-covalent proteasome inhibitors, Eur. J. Med. Chem. 76 (2014) 1−9. (e) P. Vitale, M.G. Perrone, P. Malerba, A. Lavecchia, A. Scilimati, Selective COX-11 inhibition as a target of theranostic novel diarylisoxazoles, Eur. J. Med. Chem. 74 (2014) 606−618.